4. Dynamics of Fibre Formation Processes

4.1 Task

It is well-known that textile fibres are produced with essentially three basic technologies:

a) The separating, refining, strengthening and winding up of spinnable liquid mass streams. All organic and inorganic chemical fibres are to be subsumed to this group independently, if they are produced in a melt, dry or wet spinning process.
b) The separating, parallel join and twist of fibres. All fibre yarns are to be classified into this group independently, if the single fibres come from natural (animal, vegetable) or chemical sources. The latter case is mostly extending in front of a chemical fibre spinning process as seen in case a) with following cut process.
c) Cut of plain sheets of organic polymers into thin, tape like stripes (slit film yarn).

Each fibre formation process aims at the manufacturing of yarns with equal properties along to the yarn length axis. This means in conformity with the given definitions, that all product variables, which estimate the textile processing and wear properties of the yarn, should be as constant as possible. The case of effect yarn manufacture with consciously determined periodic or stochastic disturbed yarn structures along its length axis is an exception that should be mentioned. However, it will not be subject of the following considerations.

The processing of textile yarns and their wear behaviour is characterised by the product variable mass (fineness) along the yarn length axis or deformation resistance (elastic modulus) along the fibre length axis. These product variables oscillate around their averages caused by oscillations of raw materials and process variables. Therefore these product variables characterise the yarn unevenness, in which the fineness characterises the so-called outer yarn unevenness and the elastic modulus characterises the so-called inner yarn unevenness.

4.2 Melt Spinning of Polymers

4.2.1 Variable Fibre Fineness

The yarn finenesses and the yarn orientation are the most important among the different variables which describe the yarn quality. Therefore, the development of a mathematical model for these two yarn variables should be demonstrated here. At first, we start the investigations with the variable fibre fineness.

Cause-Effect-Scheme

The cause-effect relations of the process and the product variables for the target quantity yarn fineness should be demonstrated in the following. The recommended first step of the modelling process (registration and order of relevant process and product variables; see Sect. 2.5.1) can be carried out best through the elaboration of a cause-effect-scheme. The technological scheme of a melt spinning process is shown in Fig. 4.1.

It is to be remarked that this scheme is strongly simplified. It only contains the absolutely necessary tools and variables for our considerations. For instance thread guides, the oiling system and in some cases existing godets before the winder are not drawn. It is assumed that the heating system for the spinning die is an electrical resistance heating equipment. This is usual for laboratory equipment. Typical for the polymer melt spinning process is, that the thermoplastic melt (produced normally by means of an extruder) is fed to the single spinning positions along a melt distribution system by means of an exactly feeding volume conveyor tool for each (gear pump, spinning pump). After passing the spinning die (the tool, which distributes the melt stream into the number of filaments in the yarn) the single thin melt filaments are rapidly deformed, cooled and strengthened. At this complicated rheological and structural formation, shift processes take place in the filaments, which are caused directly or indirectly by the take-up velocity, created by the winder. For the target quantity or effect variable "fineness of the spun yarn" the process and product cause variables that are probably interesting at such a spinning position are shown in Fig. 4.1 as well.
Figure 4.2 shows the cause-effect-scheme for the target quantity fineness Tt_s (designed on this basis).

The cause-effect-arrows go from the cause to the effect. The box of the target quantity fineness is thickly framed, boxes of quantities at the process periphery are shaded (from these arrows only lead off). The fineness Tt_s is only caused under static conditions from the take-down (spinning) velocity at the output of the fibre formation distance v_s and from the throughput through the spinneret Q_s, which feeds the fibre formation distance at its input. The basic equation uses the suitable dimensions

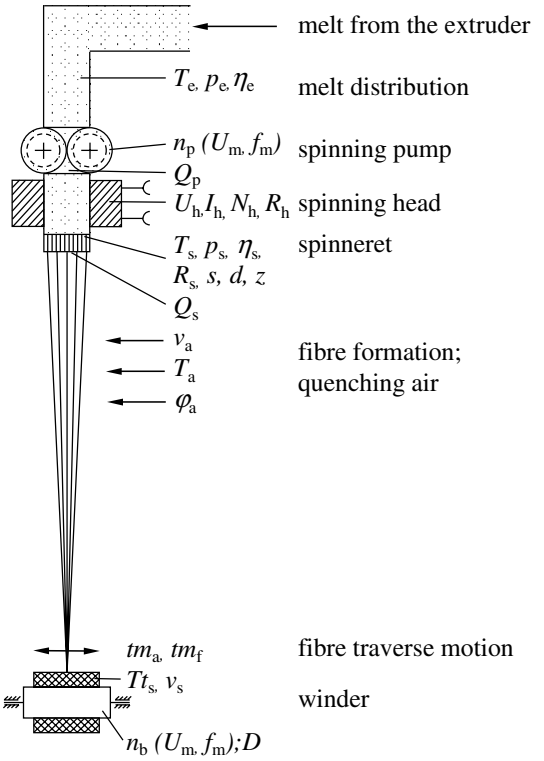

Fig. 4.1. Technological scheme (simplified) of a polymer melt spinning process

$$Tt_s[\text{tex}] = \frac{Q_s[\text{g/min}]}{v_s[\text{km/min}]} \tag{4.1}$$

It should be added, that changes of the quenching air velocity Δv_a below the die, and the necessary traverse motion at the bobbin of the winder, which is effected by the amplitude tm_a and the frequency tm_f of the thread guide for the traverse motion, also effect changes of the yarn fineness. However, they do not effect changes to the mean fineness. They only change the value of the fineness differentially. These 3 boxes are dotted frames. More detailed explanations to the latter are in Sects. 4.1.1.3 and 5.1.5.4.

The main cause variables for the fineness Tt_s, namely the throughput Q_s and the take-down (spinning) velocity v_s, can be traced back now regarding their cause process and product variables. The take-down velocity v_s is caused by the speed of the bobbin n_b, which is caused by the mains supply voltage U_m and the mains supply frequency f_m if an asynchronous drive motor is

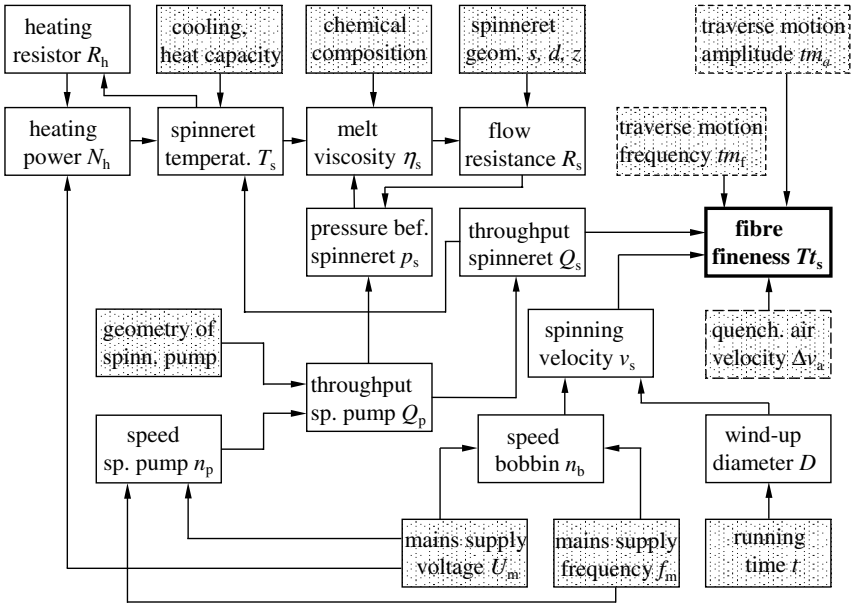

Fig. 4.2. Cause-effect-scheme for the target quantity fineness Tt_s of a polymer melt spinning process

used, and the wind-up diameter D. The latter of course increases with the running time t.

The throughput Q_s is only caused by the throughput of the spinning pump Q_p, which depends upon itself because of its geometrical design and its speed n_p. Back stream leakages of the spinning pump, which would mean $Q_s < Q_p$, are not regarded here. If the spinning pump would be driven by an asynchronous motor from the same mains supply U_m and f_m to Tt_s would be effectively doubled along the cause-effect-chains:

$$U_m,\ f_m \rightarrow n_b \rightarrow v_s \rightarrow Tt_s \text{ and}$$
$$U_m,\ f_m \rightarrow n_p \rightarrow Q_p \rightarrow Q_s \rightarrow Tt_s$$

The pressure before the spinning die p_s does not appear as a cause variable in regard to Q_s. It only depends, corresponding to the HAGEN-POISEUILLE-law for laminar flows in the tube, see [279], on the flow resistance inside the capillary holes of the die R_s and from Q_p. The flow resistance R_s depends on its part from the geometry of the capillary holes (length s, diameter d, number z) and from the melt viscosity η_s. The dependence of the melt viscosity η_s on the spinneret temperature T_s and on the chemical polymer composition is comprehensible by reason of simple basic physical laws. The dependence of T_s on the cooling conditions at the spinning die and on the heating power N_h

(itself depending on the mains supply voltage U_m and on the OHM'S heating resistance R_h) can be concluded with the same reasons.
In the next step it is necessary to set up the DEq. for each cause-effect relation or, if impossible, to investigate the dynamic signal transfer properties of the partial transfer systems. The signal transfer and signal interlacing character can be better represented by means of the so-called *functional block diagram*. In automatic control this is an often used scheme, which develops formally from the cause-effect-scheme by means of technological and *prior* physical knowledge. This only contains the change or oscillating parts of the process and product variables as their signals are connected together by cause-effect relations. The dynamic transfer properties are represented by the blocks, *"black boxes"*, which are unknown at the beginning of the analysis. This procedure will be demonstrated more fully in Sect. 4.3 with the example of "glass fibre spinning". In the following, the set up of the dynamic model will be demonstrated, which on the one hand describes the cause-effect relations between the cause variables throughput spinneret Q_s and the spinning velocity v_s and the fibre fineness Tt_s which is effected by these variables, on the other. The final goal of this procedure is to prepare technological statements about the disturbance transfer properties of the fibre formation distance.

Specified Differential Equation of a Fibre Formation Distance (simplified)

Figure 4.3 shows the fibre formation distance of the melt spinning process, only one monofilament fibre, which is reduced to the most necessary of elements and variables.

A melt stream is pressed through the capillary hole, cross section q_i, of the spinneret with the velocity v_i (input velocity or injection velocity into the fibre formation distance). At the length l between the spinneret and the take-up rolls with the output velocity v_s it is drawn, solidified and transported. The ready fibre with the cross section q_s esp. the fineness Tt_s appears at the take-up rolls. The relationship between the fibre fineness and the cross section is given by the density ϱ in the following manner:

$$Tt_s[\text{tex}] = \varrho[\text{g/cm}^3] \cdot q_s[\mu\text{m}^2] \cdot 10^{-3} \tag{4.2}$$

The following relationship exists between the mass discharge per time (or throughput) Q_s and the input variables of the fibre formation distance:

$$Q_s = \varrho \cdot q_i \cdot v_i \tag{4.3}$$

In Eq. 4.3 it is not distinguished between ϱ_{fibre} and ϱ_{melt}, because a constant factor exists between these two densities and an influence on the time and frequency oscillation relations will not be given. We split according to the

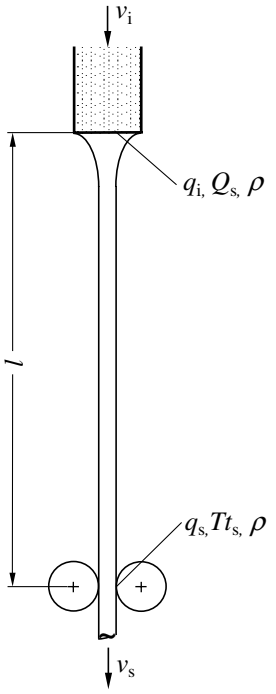

Fig. 4.3. Fibre formation distance (simplified) of the polymer melt spinning

agreement the variables, if necessary, into the mean value and the fluctuating part, consequently for instance:

$v_i = v_{im} \pm \Delta v_i$,
$q_s = q_{sm} \pm \Delta q_s$ and so on

The question is: Which Tt_s-fluctuations appear and if fluctuations of the variables v_i, q_i, ϱ, v_s or l appear? The question can only be answered on the basis of a dynamic fibre formation model. Ingeniously the starting point is the dynamic continuum equation (2.18).
Applied to the present fibre formation distance are:

mass inflow/time $= q_i \cdot v_i \cdot \varrho$
mass discharge/time $= q_s \cdot v_s \cdot \varrho = Tt_s \cdot v_s$
change of stored mass $= \dot{q}_s \cdot l \cdot \varrho = \dot{T}t_s \cdot l$

The assumed simplification at the formulation of the stored mass is, that the deformation range of the melt stream until it reaches its solidification point is not considered. At this point the diameter or the fineness of the spun fibre is reached. However, this range of the whole fibre formation distance is relatively small ($\sim$ 0.5...0.8 m), and the related mistakes do not prevent qualitatively correct results. An exact and quantitatively correct consideration of

this range makes a correct mathematical solution impossible. In Sect. 3. the very complex processes which take place in the fibre formation distance are explained in more detail.

Using the expressions above the complete DEq. of the fibre formation distance can now be written as:

$$q_\mathrm{i} \cdot v_\mathrm{i} \cdot \varrho - Tt_\mathrm{s} \cdot v_\mathrm{s} - \dot{Tt}_\mathrm{s} \cdot l = 0 \tag{4.4}$$

By marking the whole left side of the DEq. 4.4 with the letter Φ and introducing the LAPLACE-operator $p = \dfrac{\mathrm{d}}{\mathrm{d}t}$, the DEq. is converted into the transformed quantic:

$$\Phi = q_\mathrm{i} \cdot v_\mathrm{i} \cdot \varrho - Tt_\mathrm{s} \cdot v_\mathrm{s} - p \cdot Tt_\mathrm{s} \cdot l = 0 \tag{4.5}$$

Equation 4.5 represents a nonlinear DEq. first order, because all variables in the single terms, which can fluctuate, are multiplicatively connected together. Equation 4.5 can be linearised by means of the partial differentiation as follows:

$$\frac{\partial \Phi}{\partial q_\mathrm{s}} \cdot \Delta q_\mathrm{s} + \frac{\partial \Phi}{\partial v_\mathrm{s}} \cdot \Delta v_\mathrm{s} + \frac{\partial \Phi}{\partial q_\mathrm{i}} \cdot \Delta q_\mathrm{i} + \frac{\partial \Phi}{\partial v_\mathrm{i}} \cdot \Delta v_\mathrm{i} + \frac{\partial \Phi}{\partial l} \cdot \Delta l + \frac{\partial \Phi}{\partial \varrho} \cdot \Delta \varrho = 0 \tag{4.6}$$

The instruction of Eq. 4.6 means, that the whole DEq. 4.5 is to be derived partially with respect to each single variable of change. The mean value is to be set by the single derivation step for these variables which are not to be derived. The following linearised complete DEq. is achieved as the mathematical dynamic model of the fibre formation distance after the partial derivation and order of the single terms:

$$\begin{aligned} &(v_\mathrm{sm} + p \cdot l_\mathrm{m}) \cdot \Delta Tt_\mathrm{s} + Tt_\mathrm{sm} \cdot \Delta v_\mathrm{s} - v_\mathrm{im} \cdot \varrho_\mathrm{m} \cdot \Delta q_\mathrm{s} \\ &\quad - q_\mathrm{im} \cdot \varrho_\mathrm{m} \cdot \Delta v_\mathrm{i} + p \cdot Tt_\mathrm{sm} \Delta l - q_\mathrm{im} \cdot v_\mathrm{im} \cdot \Delta \varrho = 0 \end{aligned} \tag{4.7}$$

Equation 4.7 is a multilateral applicable dynamic model equation for fibre formation and fibre transport processes (see also Sect. 5.1). The performed linearisation (each term of the Eq. 4.7 contains only variables of change in time) is connected to the following consequences regarding the analysis:
Equation 4.5 represents primarily a nonlinear relationship. This is imaginable as a spatial multidimensional *curved* sheet and it is approached by a *plane* tangential sheet in the technological operating point. It is determined by the mean values of the single variables. The linearised relation is better validated the nearer the analytical investigation remains at this technological operation point. That means that the linearised Eq. 4.7 is valid more exact the smaller the investigated change quantities are in relation to their mean values. In practice it should be kept for any change variable x:

$$\Delta x \leqq 0.1 \cdot x_\mathrm{m} \tag{4.8}$$

Solutions of the Differential Equation of the Fibre Formation Process

DEq. 4.7 is the calculation basis for the characterisation of the dynamic behaviour of the fibre formation distance. It is now possible to calculate the effects of Δv_s-, Δv_i-, Δq_i-, $\Delta \varrho$- and Δl- disturbances on the fineness changes $\Delta T t_s$. Each change variable is ingeniously to be regarded separately.

Disturbance Δv_s (changes of the take-down velocity). The boundary condition for this case is:

$$\Delta v_i = \Delta q_i = \Delta \varrho = \Delta l = 0$$

Introducing this into the DEq. 4.7 and applicatiing the calculation and conversion algorithms (which were explained in detail in Sect. 2.5.2) results in:

dynamic transfer function:

$$G(p) = \frac{\Delta T t_s}{\Delta v_s} = -\frac{T t_{sm}}{v_{sm}} \cdot \frac{1}{1 + p \cdot \dfrac{l_m}{v_{sm}}} \tag{4.9}$$

The *complex frequency response* follows:

$$G(j\omega) = \frac{\widetilde{\Delta T t_s}}{\widetilde{\Delta v_s}} \cdot e^{j\varphi} = -\frac{T t_{sm}}{v_{sm}} \cdot \frac{1}{1 + j\omega \cdot \dfrac{l_m}{v_{sm}}} \tag{4.10}$$

Equation 4.10 can be split into the *amplitude frequency response* (simply also *amplitude response*)

$$|G(j\omega)| = \left| \frac{\widetilde{\Delta T t_s}}{\widetilde{\Delta v_s}} \right| = (-)\frac{T t_{sm}}{v_{sm}} \left[1 + \left(\omega \cdot \frac{l_m}{v_{sm}} \right)^2 \right]^{-1/2} \tag{4.11}$$

and the *phase frequency response* (simply *phase response*)

$$\varphi(\omega) = \arctan \left[-\frac{\omega \cdot l_m}{v_{sm}} \right] - \pi \tag{4.12}$$

By means of Eqs. 4.9 and 2.41 the *time transient function* can be calculated as: (also *step response*)

$$\underline{\Delta T t_s} | \overline{\Delta v_s} = -\Delta v_s \cdot \frac{T t_{sm}}{v_{sm}} \left[1 - \exp \left(-\frac{v_{sm}}{l_m} \cdot t \right) \right] \tag{4.13}$$

A collected qualitative and quantitative evaluation of the results of Eqs. 4.9 to 4.13 is given in the next Sect. *"Summarised Evaluation and Conclusions to the Solutions of the Differential Equation"*. However, already here

it should be referred to the minus sign in the Eqs. 4.9, 4.10, 4.11, 4.13, which hints at the physical right dependence: A positive Δv_s-change effects a negative $\Delta T t_\mathrm{s}$-change. That means an *increase* of the take-down velocity effects, under constant other conditions, a *decrease* of the spun fibre fineness.

Disturbance Δv_i (changes of the input velocity). Boundary condition:

$$\Delta v_\mathrm{s} = \Delta q_\mathrm{i} = \Delta \varrho = \Delta l = 0$$

It is to be written in the same manner as described before:

dynamic transfer function:

$$G(p) = \frac{\Delta T t_\mathrm{s}}{\Delta v_\mathrm{i}} = \frac{q_\mathrm{i} m \cdot \varrho_\mathrm{m}}{v_\mathrm{sm}} \cdot \frac{1}{1 + p \cdot \dfrac{l_\mathrm{m}}{v_\mathrm{sm}}} \tag{4.14}$$

or, because $q_\mathrm{im} \cdot \varrho_\mathrm{m} = T t_\mathrm{sm} \cdot \dfrac{v_\mathrm{sm}}{v_\mathrm{im}}$

$$G(p) = \frac{\Delta T t_\mathrm{s}}{\Delta v_\mathrm{i}} = \frac{T t_\mathrm{sm}}{v_\mathrm{im}} \cdot \frac{1}{1 + p \cdot \dfrac{l_\mathrm{m}}{v_\mathrm{sm}}} \tag{4.15}$$

complex frequency response:

$$G(\mathrm{j}\omega) = \frac{\widetilde{\Delta T t_\mathrm{s}}}{\widetilde{\Delta v_\mathrm{i}}} \cdot \mathrm{e}^{\mathrm{j}\varphi} = \frac{T t_\mathrm{sm}}{v_\mathrm{im}} \cdot \frac{1}{1 + \mathrm{j}\omega \cdot \dfrac{l_\mathrm{m}}{v_\mathrm{sm}}} \tag{4.16}$$

amplitude frequency response (simply also *amplitude response*)

$$|G(\mathrm{j}\omega)| = \left| \frac{\widetilde{\Delta T t_\mathrm{s}}}{\widetilde{\Delta v_\mathrm{i}}} \right| = \frac{T t_\mathrm{sm}}{v_\mathrm{im}} \left[1 + \left(\omega \cdot \frac{l_\mathrm{m}}{v_\mathrm{sm}} \right)^2 \right]^{-1/2} \tag{4.17}$$

phase frequency response (simply *phase response*)

$$\varphi(\omega) = \arctan \left[-\frac{\omega \cdot l_\mathrm{m}}{v_\mathrm{sm}} \right] \tag{4.18}$$

time transient function (or *step response*)

$$\underline{\Delta T t_\mathrm{s}} | \overline{\Delta v_\mathrm{i}} = \Delta v_\mathrm{i} \cdot \frac{T t_\mathrm{sm}}{v_\mathrm{im}} \left[1 - \exp \left(-\frac{v_\mathrm{sm}}{l_\mathrm{m}} \cdot t \right) \right] \tag{4.19}$$

A collected qualitative and quantitative evaluation of the result Eqs. 4.15 to 4.19 is given in the next Sect. *"Summarised Evaluation and Conclusions to the Solutions of the Differential Equation"*. The effects of Δv_i-disturbances are

co-directional to the ΔTt_s-changes opposite to the described Δv_s-disturbances. That means an *increase* of the input velocity effects under constant other conditions, an *increase* of the spun fibre fineness as well. Besides it should also be hinted here, that the result equations of Sect. 2.5.2 (example drawing process at input velocity disturbances) are equivalent to the presented result equations of the fibre formation distance for Δv_i-disturbances. That means it corresponds in each case Eqs. 4.15 to 2.40, 4.16 to 2.36, 4.17 to 2.38, 4.18 to 2.39 and 4.19 to 2.46.

Disturbance Δq_i (changes of the input cross sectional area). Boundary condition:

$$\Delta v_\mathrm{s} = \Delta v_\mathrm{i} = \Delta \varrho = \Delta l = 0$$

Such a disturbance is actually unlikely for a melt spinning process (it would be more plausible to assume step-like or oscillating changes of the capillary hole diameter in the spinneret). Nevertheless, dynamic solution equations will be explained in the following for this disturbance model as well. In a row of other fibre formation and fibre processing processes Δq_i-disturbances are identical namely with changes of the fineness at the process input. A modified application of the here given result equations is easily possible. Examples will follow in later sections.

dynamic transfer function:

$$G(p) = \frac{\Delta Tt_\mathrm{s}}{\Delta q_\mathrm{i}} = \varrho_\mathrm{m} \cdot \frac{v_\mathrm{im}}{v_\mathrm{sm}} \cdot \frac{1}{1 + p \cdot \dfrac{l_\mathrm{m}}{v_\mathrm{sm}}} \tag{4.20}$$

or, because $v_\mathrm{im} \cdot \varrho_\mathrm{m} = \dfrac{Tt_\mathrm{sm} \cdot v_\mathrm{sm}}{q_\mathrm{im}}$

$$G(p) = \frac{\Delta Tt_\mathrm{s}}{\Delta q_\mathrm{i}} = \frac{Tt_\mathrm{sm}}{q_\mathrm{im}} \cdot \frac{1}{1 + p \cdot \dfrac{l_\mathrm{m}}{v_\mathrm{sm}}} \tag{4.21}$$

complex frequency response:

$$G(\mathrm{j}\omega) = \frac{\widetilde{\Delta Tt_\mathrm{s}}}{\widetilde{\Delta q_\mathrm{i}}} \cdot \mathrm{e}^{\mathrm{j}\varphi} = \frac{Tt_\mathrm{sm}}{q_\mathrm{im}} \cdot \frac{1}{1 + \mathrm{j}\omega \cdot \dfrac{l_\mathrm{m}}{v_\mathrm{sm}}} \tag{4.22}$$

amplitude frequency response (simply also *amplitude response*)

$$|G(\mathrm{j}\omega)| = \left| \frac{\widetilde{\Delta Tt_\mathrm{s}}}{\widetilde{\Delta q_\mathrm{i}}} \right| = \frac{Tt_\mathrm{sm}}{q_\mathrm{im}} \left[1 + \left(\omega \cdot \frac{l_\mathrm{m}}{v_\mathrm{sm}} \right)^2 \right]^{-1/2} \tag{4.23}$$

phase frequency response (simply *phase response*)

$$\varphi(\omega) = \text{arc tan}\left[-\frac{\omega \cdot l_\text{m}}{v_\text{sm}}\right] \tag{4.24}$$

time transient function (or *step response*)

$$\underline{\Delta T t_\text{s}}|\overline{\Delta q_\text{i}} = \Delta q_\text{i} \cdot \frac{T t_\text{sm}}{q_\text{im}}\left[1 - \exp\left(-\frac{v_\text{sm}}{l_\text{m}} \cdot t\right)\right] \tag{4.25}$$

A collected qualitative and quantitative evaluation of the result of Eqs. 4.21 to 4.25 is given in the next Sect. *"Summarised Evaluation and Conclusions to the Solutions of the Differential Equation"*. But, it should already be said here, that the effected $\Delta T t_\text{s}$-disturbances, caused by Δq_i-disturbances, are co-directional.

Disturbance $\Delta\varrho$ (changes of the density of fibre material). Boundary condition:

$$\Delta v_\text{s} = \Delta v_\text{i} = \Delta q_\text{i} = \Delta l = 0$$

It can be concluded in the same manner as described before:

dynamic transfer function:

$$G(p) = \frac{\Delta T t_\text{s}}{\Delta\varrho} = \frac{q_\text{im} \cdot v_\text{im}}{v_\text{sm}} \cdot \frac{1}{1 + p \cdot \dfrac{l_\text{m}}{v_\text{sm}}} \tag{4.26}$$

or, because $q_\text{im} \cdot v_\text{im} = \dfrac{T t_\text{sm} \cdot v_\text{sm}}{\varrho_\text{m}}$

$$G(p) = \frac{\Delta T t_\text{s}}{\Delta\varrho} = \frac{T t_\text{sm}}{\varrho_\text{m}} \cdot \frac{1}{1 + p \cdot \dfrac{l_\text{m}}{v_\text{sm}}} \tag{4.27}$$

complex frequency response:

$$G(\text{j}\omega) = \frac{\widetilde{\Delta T t_\text{s}}}{\widetilde{\Delta\varrho}} \cdot \text{e}^{\text{j}\varphi} = \frac{T t_\text{sm}}{\varrho_\text{m}} \cdot \frac{1}{1 + \text{j}\omega \cdot \dfrac{l_\text{m}}{v_\text{sm}}} \tag{4.28}$$

amplitude frequency response (simply also *amplitude response*)

$$|G(\text{j}\omega)| = \left|\frac{\widetilde{\Delta T t_\text{s}}}{\widetilde{\Delta\varrho}}\right| = \frac{T t_\text{sm}}{\varrho}\left[1 + \left(\omega \cdot \frac{l_\text{m}}{v_\text{sm}}\right)^2\right]^{-1/2} \tag{4.29}$$

phase frequency response (simply *phase response*)

$$\varphi(\omega) = \text{arc tan}\left[-\frac{\omega \cdot l_\text{m}}{v_\text{sm}}\right] \tag{4.30}$$

time transient function (or *step response*)

$$\underline{\Delta T t_\text{s}}|\overline{\Delta\varrho} = \Delta\varrho \cdot \Delta\varrho \cdot \frac{T t_\text{sm}}{\varrho_\text{m}}\left[1 - \exp\left(-\frac{v_\text{sm}}{l_\text{m}} \cdot t\right)\right] \tag{4.31}$$

A co-directional dependence of $\Delta\varrho$-changes on effected $\Delta T t_\text{s}$-changes is also to be seen here. A collected qualitative and quantitative evaluation of the result of Eqs. 4.27 to 4.31 is given in the next Sect. *"Summarised Evaluation and Conclusions to the Solutions of the Differential Equation"*.

Disturbance Δl (changes of the length of the fibre formation distance). Boundary condition:

$$\Delta v_\text{s} = \Delta v_\text{i} = \Delta q_\text{i} = \Delta\varrho = 0$$

At first glance, this disturbance does not seem to be of any practical interest. But it is to be hinted, that the fibre influence by means of the dynamics of thread traverse motion at winders (especially at the godetless high speed melt spinning) is exactly equivalent to the change model *"length of the fibre formation distance"*. More details can be found in Sect. 5.1.5.

The following result equations are to be concludet:

dynamic transfer function:

$$G(p) = \frac{\Delta T t_\text{s}}{\Delta l} = -\frac{T t_\text{sm}}{l_\text{m}} \cdot \frac{p}{p + \dfrac{v_\text{sm}}{l_\text{m}}} \tag{4.32}$$

complex frequency response:

$$G(\text{j}\omega) = \frac{\widetilde{\Delta T t_\text{s}}}{\widetilde{\Delta l}} \cdot \text{e}^{\text{j}\varphi} = -\frac{T t_\text{sm}}{l_\text{m}} \cdot \frac{\text{j}\omega}{\text{j}\omega + \dfrac{v_\text{sm}}{l_\text{m}}} \tag{4.33}$$

amplitude frequency response (simply also *amplitude response*)

$$|G(\text{j}\omega)| = \left|\frac{\widetilde{\Delta T t_\text{s}}}{\widetilde{\Delta l}}\right| = (-)\frac{T t_\text{sm}}{l_\text{m}} \cdot \omega \cdot \left[\omega^2 + \left(\frac{v_\text{sm}}{l_\text{m}}\right)^2\right]^{-1/2} \tag{4.34}$$

phase frequency response (simply *phase response*)

$$\varphi(\omega) = \text{arc tan}\left[\frac{v_{\text{sm}}}{\omega \cdot l_{\text{m}}}\right] - \pi \tag{4.35}$$

time transient function (or *step response*)

$$\underline{\Delta T t_{\text{s}}}|\overline{\Delta l} = -\Delta l \cdot \frac{T t_{\text{sm}}}{l_{\text{m}}} \cdot \exp\left(-\frac{v_{\text{sm}}}{l_{\text{m}}} \cdot t\right) \tag{4.36}$$

Also these result Eqs. 4.32 to 4.36 will be collected and discussed in the following Sect. *"Summarised Evaluation and Conclusions to the Solutions of the Differential Equation"*

Summarised Evaluation and Conclusions to the Solutions of the Differential Equation

Three summarised unifying statements can be made by the comparing all result equations regarding the cause-effect relations between the different process and product variables Δv_{s}, Δv_{i}, Δq_{i}, $\Delta \varrho$ and Δl on the one hand and the product variable $\Delta T t_{\text{s}}$ on the other:

1. Statement

Four of the five dynamic transfer functions are equally constructed. (cp. 4.9, 4.15, 4.21 and 4.27). This fact leads of course to equally constructed, from it derived functions, as complex frequency response, amplitude frequency response, phase frequency response and step response. This applies to the disturbances Δv_{s}, Δv_{i}, Δq_{i} and $\Delta \varrho$. This dynamic behaviour is characterised by it in the transfer function, that the LAPLACE-operator p exists only once linear in one of two terms of the denominator. Such a behaviour is called proportional action with delay of first order. It is typical for such a system behaviour, that residual changes (esp. step-like) of the cause variables (if they continue long enough) effect residual changes of the effect variables ($\Delta T t_{\text{s}}$), in which the quantities of cause and effect changes are proportional to each other. Delay of first order means, that only *one* time constant and only *one* exponential function (coming from only *one* differential quotient in the DEq.) determine the dynamic transient process.

2. Statement

The dynamic transfer function for the disturbance Δl (Eq. 4.32) is deflectively constructed. It actually possesses the same denominator compared with the named transfer functions in the first statement, but the LAPLACE-operator p appears once more linear in the numerator. This behaviour is

called differential action with delay of first order. It is typical for such a system behaviour, that changes of the effect variables ($\Delta T t_s$) reduce to zero again, if the changes(esp. step-like) of the cause variables only continue long enough. Delay of first order means in this case, that likewise only *one* time constant and only *one* exponential function determine the subsidence of the effect to zero (a transient process as well).

3. Statement

The dynamic behaviour of a fibre formation distance is dominated by the quantity l_m/v_{sm}. This was also the case in Sect. 2.5.2 (there for the drawing process) for the system time constant T_c (see Eq. 2.47). The time constant T_c is readable from the exponent of the e-functions in the time transient functions of Eqs. 4.13, 4.19, 4.25, 4.31 and 4.36.
The critical frequency f_c can be determined likewise by l_m and v_{sm} corresponding to Eq. 2.49 (v_{sm} corresponds to v_{om}).

Considering the first statement it is possible to get common solutions for the four disturbance causes Δv_s, Δv_i, Δq_i and $\Delta \varrho$ regarding their effects to the fineness $\Delta T t_s$. Uniform, normalised solutions can be determined for the complex frequency response, the amplitude frequency response, the phase frequency response and the time transient function (step response), which are valid for all of the four disturbance causes in similar manners.

Considering Eqs. 2.48 and 2.49 one gets from the Eqs. 4.10, 4.16, 4.22 and 4.28 the *common normalised complex frequency response*, in which ω is substituted by f:

$$\begin{aligned} G[\mathrm{j}(f/f_c)] &= -\frac{\widetilde{\Delta T t_s}/T t_{sm}}{\widetilde{\Delta v_s}/v_{sm}} \cdot e^{\mathrm{j}\varphi} = \frac{\widetilde{\Delta T t_s}/T t_{sm}}{\widetilde{\Delta v_i}/v_{im}} \cdot e^{\mathrm{j}\varphi} \\ &= \frac{\widetilde{\Delta T t_s}/T t_{sm}}{\widetilde{\Delta q_i}/q_{im}} \cdot e^{\mathrm{j}\varphi} = \frac{\widetilde{\Delta T t_s}/T t_{sm}}{\widetilde{\Delta \varrho}/\varrho_m} \cdot e^{\mathrm{j}\varphi} \\ &= \frac{\mathbf{1}}{\mathbf{1 + j(f/f_c)}} \end{aligned} \tag{4.37}$$

Considering Eqs. 2.48 and 2.49 one gets from the Eqs. 4.11, 4.17, 4.23 and 4.29 in the same manner the *common normalised amplitude frequency response*:

$$\begin{aligned} |G[\mathrm{j}(f/f_c)]| &= \left| \frac{\widetilde{\Delta T t_s}/T t_s m}{\widetilde{\Delta v_s}/v_{sm}} \right| = \left| \frac{\widetilde{\Delta T t_s}/T t_s m}{\widetilde{\Delta v_i}/v_{im}} \right| \\ = \left| \frac{\widetilde{\Delta T t_s}/T t_s m}{\widetilde{\Delta q_i}/q_{im}} \right| &= \left| \frac{\widetilde{\Delta T t_s}/T t_s m}{\widetilde{\Delta \varrho}/\varrho_m} \right| = \mathbf{[1 + (f/f_c)^2]^{-1/2}} \end{aligned} \tag{4.38}$$

The *transfer locus* of this normalised complex frequency response is shown in Fig. 4.4.

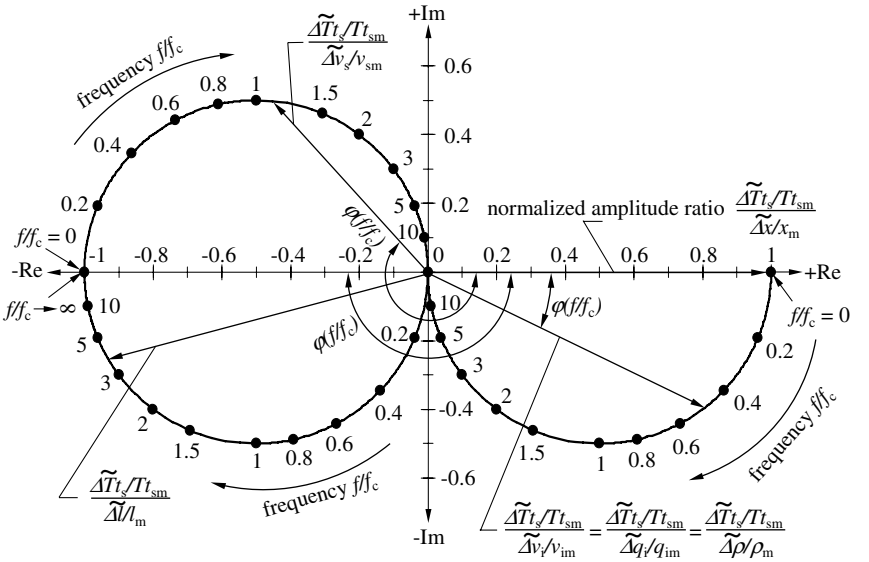

Fig. 4.4. Transfer locus of the normalised complex frequency responses for changes of fibre fineness $\Delta T t_s$ in consequence of different disturbance causes (Eqs. 4.37 and 4.42)

It should be considered that, at the modulus generation the negative sign for the disturbance Δv_s disappears. The normalised amplitude frequency response is presented in Fig. 4.5.

The *common normalised phase frequency response* of the same single phase frequency responses of Eqs. 4.18, 4.24 and 4.30 is:

$$\varphi(f) = \text{arc tan}[-f/f_c] \tag{4.39}$$

and for 4.12:

$$\varphi(f) = \text{arc tan}[-f/f_c] - \pi \tag{4.40}$$

Both are also included in Fig. 4.5. At last the *common normalised step responses* can be concluded from Eqs. 4.13, 4.19, 4.25 and 4.29 considering Eq. 2.48:

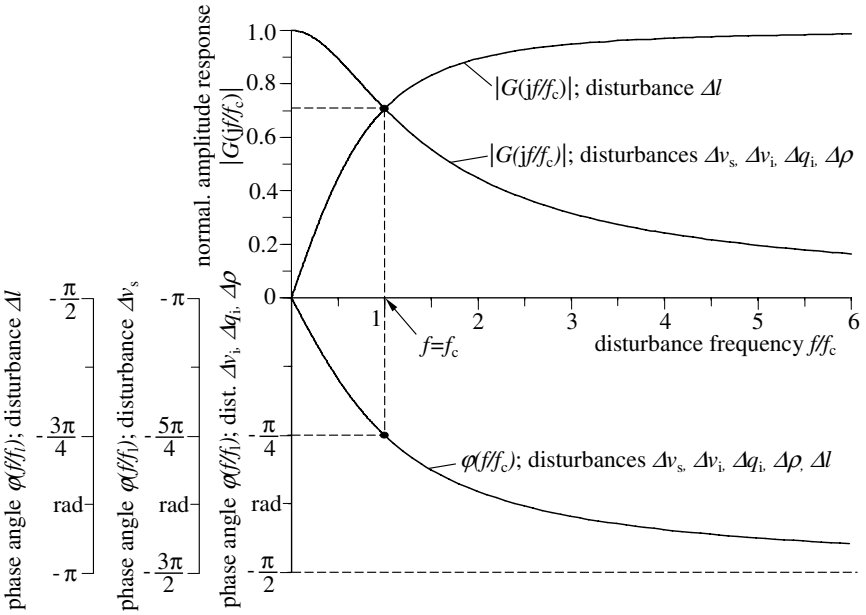

Fig. 4.5. Normalised amplitude frequency responses and normalised phase frequency responses for changes of fibre fineness $\Delta T t_s$ in consequence of different disturbance causes (Eqs. 4.38 and 4.43 as well as 4.39, 4.40 and 4.44)

$$\begin{aligned}\frac{-\Delta T t_s/T t_{sm}\overline{|\Delta v_s|}}{\Delta v_s/v_{sm}} &= \frac{\Delta T t_s/T t_{sm}\overline{|\Delta v_i|}}{\Delta v_i/v_{im}} \\ = \frac{\Delta T t_s/T t_{sm}\overline{|\Delta q_i|}}{\Delta q_i/q_{im}} &= \frac{\Delta T t_s/T t_{sm}\overline{|\Delta \varrho|}}{\Delta \varrho/\varrho_m} \\ &= \mathbf{1} - \exp(\mathbf{-}\boldsymbol{t}/\boldsymbol{T_c})\end{aligned} \tag{4.41}$$

The common normalised step response is shown in Fig. 4.6. It is characteristic for this type of disturbances, that the effect to the fibre fineness is smaller the smaller the disturbance frequency f is. In a way steady state Δl-changes (frequency $f \approx 0$) do not result in fineness changes (see Figs. 4.4 and 4.5), whereas the frequency and amplitude frequency responses rapidly approach the maximum amplification factor 1 for $f > f_c$.
This differential action appears in the step response. The fineness shift is first of all a maximum after the imprint of the cause step Δl and after that decreases to zero according to e^{-t/T_c}. The critical frequency f_c or the time constant of the system T_c are the significant sizes for quantitative estimations here as well.

Quantitative conditions can be deduced easily, for instance from the developed relationships for the design of yarn traverse motion systems at wind-up devices. The goal is in this case a minimising of the fineness changes $\Delta T t_s$,

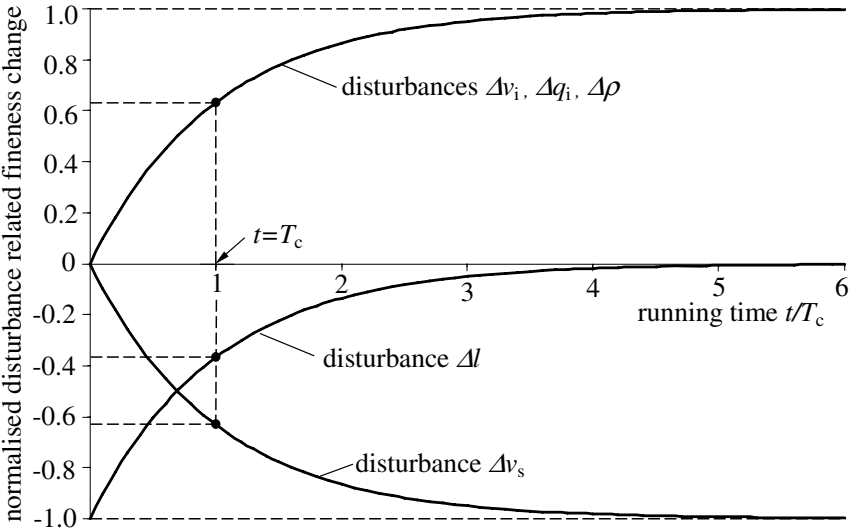

Fig. 4.6. Normalised step response for changes of fibre fineness $\Delta T t_s$ in consequence of different disturbance causes (Eqs. 4.41 and 4.45)

caused by the permanent effecting Δl-changes (see example presentation in Sect. 5.1.5). A high critical frequency f_c (that means short fibre formation distances l_m and high take-up velocities v_{om}) would be preferred for the disturbance type Δl alone. However, these are conditions which are connected with high amplifications of the other dealt with disturbance causes. At this point it is necessary that compromises be settled.

More remarks to the phase frequency responses of the dealt with disturbance causes (Fig. 4.5):

The disturbances Δv_i, Δq_i, and $\Delta\varrho$ result in the running behind of the phase shift angles of the effect oscillations against the periodic cause oscillations (they start for $f/f_c = 0$ with $\varphi = 0$ and end for $f/f_c \to \infty$ with $\varphi = -\pi/2$). Whereas, the disturbance Δv_s causes (settled by the negative coupling to the effect oscillation $\Delta T t_s$ - see the minus signs before the functions in Eqs. 4.9 until 4.11 and 4.13) a running behind of the phase shift angle which is additionally shifted about $-\pi$. That means it starts for $f/f_c = 0$ with $\varphi = -\pi$ and ends for $f/f_c \to \infty$ with $\varphi = -3\pi/2$ (see also Eq. 4.12).

A differential action with delay of first order (in the present case Δl-disturbances) normally results in a running before of the phase shift angles which start at $f/f_c = 0$ with $\varphi = +\pi/2$ and end for $f/f_c \to \infty$ with $\varphi = 0$. Because the coupling between the Δl-disturbances and the effected $\Delta T t_s$-disturbances is also negative (minus signs before the functions in

Eqs. 4.32...4.34 and 4.36) the phase shift angles are shifted in the same way about $-\pi$ (see also Eq. 4.35). The result is the altogether running behind of the phase shift angles, which appear as $\varphi = -\pi/2$ (for $f/f_c = 0$) until $\varphi = -\pi$ (for $f/f_c \to \infty$).

These specialities for Δv_s- and Δl-disturbances are considered in Fig. 4.5 by different ordinates for the common dotted drawn phase frequency response curve.

Further explanations to the use of the phase frequency response for the analysis of specific problems will be given in Sect. 5.1.5.

The system time constant T_c and the critical frequency f_c of a fibre formation distance respectively a fibre formation line (we will see later that it is also valid for many yarn processing lines in the same manner), which are characterised by a length l_m, can be investigated by means of the nomogram in Fig. 4.7. These lines are characterised by a length of l_m which passes the fibre or yarn with the output or take-up velocity v_{om}. The nomogram is the graph of the definition of Eqs. 2.47 and 2.49 and allows for a quick estimation of T_c and f_c. l_m and v_{om} (outer ladders) are to be lined rectilinearly and T_c and f_c can be read from the point of intersection with the middle ladder. The drawn straight lines (1) and (2) represent the concrete application examples that have been described in Sects. 2.5.2 and 5.1.5.

As one can see, the ordinates of Figs. 4.5 and 4.6 are divided appropriately into the dimensionless ratio of relative effect-cause-changes, and the abscissa is divided into the also dimensionless ratio f/f_c or t/T_c. The ordinate values assert, by which factor a percentage cause change is to be multiplied in order to get the effected fineness change. This factor is at the most 1 for small disturbance frequencies (periodic disturbances) or for infinite long times (step-like disturbances). If the frequency of the disturbances is exactly equal to the critical frequency of the fibre formation distance ($f = f_c$) then the factor is $1/\sqrt{2} \approx 0.71$ and decreases with greater disturbance frequency quickly to zero.
Normally disturbances should only influence the aim variable as little as possible. Taking this into consideration the technological operating point of the fibre formation distance demands that the time constant T_c should be as much as possible and concerning the critical frequency f_c as little as possible. It is then guaranteed, that disturbances of small frequency no longer have any considerable penetrance to the aim variable fibre fineness. It is to be reached, if either the length of the fibre formation distance l_m can be enlarged and/or the take-up (spinning) velocity v_{sm} can be reduced. The latter is not usually desired. But this dynamic model reflection shows that the instable process behaviour at increased velocity is objectively foundable on the one

hand. It also shows on the other the limits of constructive and technological compromises, which can be made if necessary.

The cause-effect-transmission of the disturbance model Δl is the exact opposite of the four dealt with disturbance models above. The normalised complex frequency response can be concluded from Eq. 4.33 considering Eqs. 2.48 and 2.49:

$$G(\mathrm{j}f) = \frac{\widetilde{\Delta T t_\mathrm{s}}/T t_\mathrm{sm}}{\widetilde{\Delta l_\mathrm{s}}} \cdot e^{\mathrm{j}\varphi} = -\frac{j(f/f_\mathrm{c})}{1 + j(f/f_\mathrm{c})} \tag{4.42}$$

The transfer locus of this normalised complex frequency response is also included in Fig. 4.4.
One can get the amplitude frequency response from Eq. 4.34 in the same manner considering Eqs. 2.48 and 2.49:

$$|G(\mathrm{j}f)| = \left| \frac{\widetilde{\Delta T t_\mathrm{s}}/T t_\mathrm{sm}}{\widetilde{\Delta l_\mathrm{s}}} \right| = (-)(f/f_\mathrm{c}) \left[1 + (f/f_\mathrm{c})^2\right]^{-1/2} \tag{4.43}$$

The normalised phase frequency response is according to 4.35:

$$\varphi(f) = \text{arc tan}(f_\mathrm{c}/f) - \pi \tag{4.44}$$

Normalised amplitude and phase frequency responses are shown in Fig. 4.5. The minus sign of the complex frequency response is suppressed in the modulus representation of the amplitude frequency response. At quantitative evaluations it has to be considered of course, that a positive Δl-change correlates with a negative $\Delta T t_\mathrm{s}$-change and vice versa.
At last from Eq. 4.36 we get the step response as:

$$\frac{\Delta T t_\mathrm{s}/T t_\mathrm{sm}|\overline{\Delta l}}{\Delta l/l_\mathrm{m}} = -\exp(-t/T_\mathrm{c}) \tag{4.45}$$

This normalised step response is shown in Fig. 4.6.

It is characteristic of this kind of disturbance, that the effect to the fibre fineness is smaller if the frequency f of disturbances is smaller. In a way steady state Δl-changes (frequency $f \approx 0$) result in no fineness changes whatsoever (see Figs. 4.4 and 4.5), whereas the frequency and amplitude frequency responses quickly reach the maximum amplification factor 1 for $f > f_\mathrm{c}$.

This differential action is expressed in the presentation of the step response (Fig. 4.6) so that an imprinted step Δl causes first of all a maximum fineness shift, which then decreases to zero according to $\exp(-t/T_\mathrm{c})$. The critical frequency f_c or the system time constant T_c are significant quantities also for quantitative estimations in such cases.

The developed relationships can be used for instance as the calculation basis for the design of traverse motion systems at winders. It is possible to give quantitative conditions for a reduction of the fineness changes $\Delta T t_s$ caused by the permanent effecting Δl-changes (see example in Sect. 5.1.5). A high critical frequency f_c would be preferred for the disturbance type Δl, this means a short fibre formation distance l_m and a high take-up velocity v_{om} would be favourable. However, these are just conditions for a high amplification of the other dealt with disturbance causes as named before. The necessity of compromises is obvious at this point.

A few remarks to the phase frequency responses of the dealt with disturbance causes (Fig. 4.5):

The disturbances $\Delta v_i, \Delta q_i$ and $\Delta \varrho$ produce running behind phase shift angles versus the causing oscillations ($f/f_c = 0$ starts with $\varphi = 0$ and ends for $f/f_c \to \infty$ with $\varphi = -\pi/2$). Whereas, the disturbance Δv_s (involved by the negative coupling to the effected oscillation $\Delta T t_s$ - see minus signs before the dynamic functions of Eqs. 4.9 to 4.11 and 4.13) produces a running behind phase shift angle which is shifted additionally by $-\pi$. This means, it starts with $f/f_c = 0$ with $\varphi = -\pi$ and ends with $f/f_c \to \infty$ with $\varphi = -3\pi/2$ (see also Eq. 4.12).

A differential action with delay of first order (as being submitted by the disturbance Δl) normally produces running before phase shift angles which start with $f/f_c = 0$ with $\varphi = +\pi/2$ and ends with $f/f_c \to \infty$ with $\varphi = 0$. But, also because a negative coupling is given for Δl-disturbances to the effected $\Delta T t_s$-disturbances (see minus signs before the dynamic functions of Eqs. 4.32 to 4.34 and 4.36) the phase shift angles are also shifted by $-\pi$ (see also Eq. 4.35). Therefore, running behind phase shift angles appear altogether which start with $\varphi = -\pi/2$ (for $f/f_c = 0$) and end with $\varphi = -\pi$ (for $f/f_c \to \infty$). These specialities by Δv_s- and Δl-disturbances are considered in Fig. 4.5 by different ordinates for the dotted lined common phase frequency response. More detailed explanations to the use of the phase frequency response for special problems will be given in Sect. 5.1.5.

The system time constant T_c and the critical frequency f_c of a fibre formation distance (we will see later, that it is also valid for many other fibre processing distances) can be found out by means of the nomogram Fig. 4.7. This converts the Eqs. 2.47 and 2.49 into a quickly utilisable manner. To this the length of the fibre formation distance l_m and the take-up velocity v_{om} (outer nomogram ladders) are connected rectilinearly and in the cross point with the middle ladder the T_c and/or f_c can be read. This is done for instance for two applications, dealt with in Sects. 2.5.2 and 5.1.5 (straight lines (1) and (2)).

At last some remarks to the question of the model-mathematical treatment of different process and product variable disturbances which simultane-

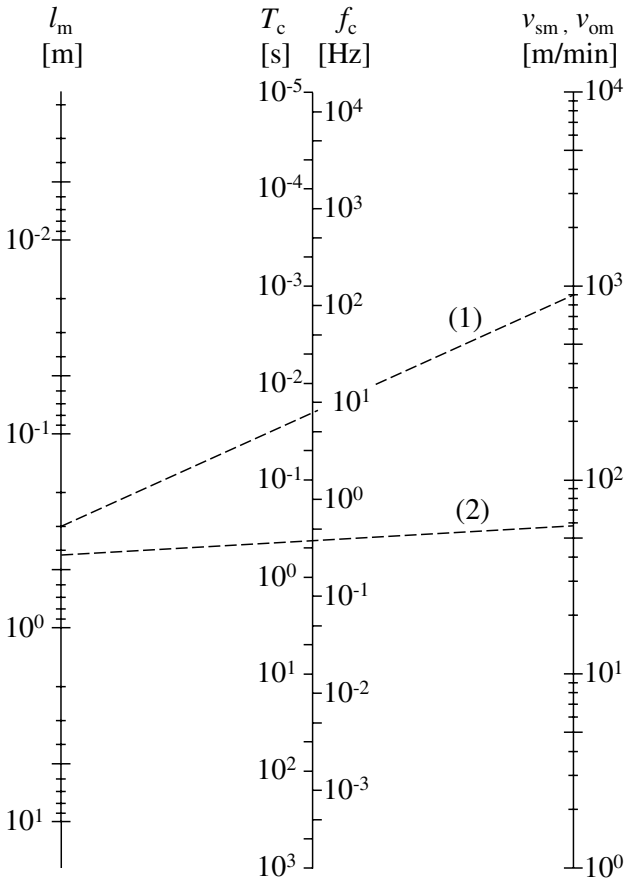

Fig. 4.7. Nomogram to the estimation of the time constant T_c and of the critical frequency f_c for fibre formation and fibre processing processes;
example (1): drawing process; v_{om}=900 m/min, l_m=0.3 m, T_c=0.02 s, f_c=8 Hz
example (2): length of the yarn input distance on a twister; v_{om}=58 m/min, l_m=0.42 m, T_c=0.43 s, f_c=0.37 Hz

ously appear and effect fibre fineness changes. In principle, the superposition principle can be applied to the single developed solution equations (transfer function, complex frequency response and time transient function) for the single disturbance of the DEq. 4.7. However, the following has be taken into consideration:

a) The related step response (for instance Eqs. 4.13 and 4.19, if step-like disturbances Δv_s and Δv_i are at hand) are added in consideration of the time range. If the different disturbances do not start at the same time $t = 0$ then the corresponding time shift of the one transient function to the other is to

be considered. Of course a graphic addition of the transient functions is also possible.

b) The related dynamic transfer functions or complex frequency responses (for instance Eqs. 4.9 and 4.15 or 4.10 and 4.16, if periodic disturbances $\widetilde{\Delta v_\mathrm{s}}$ and $\widetilde{\Delta v_\mathrm{i}}$ are at hand) are to be added corresponding to the rules of the addition of complex numbers (vector addition) in consideration of the frequency range. If the exciting frequency ω is not the same for the viewed disturbances then ω_1 and ω_2 must be put in separately to both basic equations of the complex frequency responses (corresponding to $p_1 = \mathrm{j}\omega_1$ and $p_2 = \mathrm{j}\omega_2$ to both basic equations of the transient functions). The amplitude frequency responses and the phase frequency responses can only be calculated by means of the complex added complex frequency responses and not by means of the simple addition of the amplitude and phase frequency responses from the both single disturbances.

4.2.2 Variable Fibre Orientation

Cause-Effect-Scheme

A very important product variable of a melt spun fibre is the achieved orientation of the macromolecules along the fibre length axis, consequently along the main tension direction during the fibre formation and elongation processes. The orientation determines the textile-physical properties of the fibre decisively. This fibre orientation determines the breaking tensile force F_b and the breaking elongation ε_b. It should be characterised by the orientation elongation ε_o which the fibre has suffered, starting from the complete unsettled isotropic state of the thermoplastic melt. A measurement for ε_o is the birefringence of the fibre Δ_o at the exit of a special fibre formation distance.

The following a-priori knowledges from the literature [280, 281] are important and are concerned with the qualitative and quantitative relationship between the imprinted orientation elongation ε_o and the causing process and product variables in the fibre formation process:

a) Thermoplastic fibre polymers possess a maximum imprintable orientation elongation $\varepsilon_\mathrm{omax}$. This is independent of the kind and the quantity of as to time consecutive elongation steps (spinning, draw and tensile testing or high speed spinning, post draw and tensile testing and so on) and its value is nearly constant for an appointed fibre polymer.

If the achieved elongation ε_oi of a single elongation step i is expressed as the natural logarithm, consequently:

$$\varepsilon_\mathrm{oi} = \ln\left[\frac{Tt_\mathrm{ii}}{Tt_\mathrm{oi}}\right]$$

then it is valid with good exactness for the fibre material PA

$$\varepsilon_{oi} = \sum_{i=1}^{n} \varepsilon_{oi} \approx 2$$

and for the fibre material PET

$$\varepsilon_{oi} = \sum_{i=1}^{n} \varepsilon_{oi} \approx 2.3$$

b) In the first step of such a consecutive chain of elongation steps (this is the spinning step) the fibre has reached the orientation elongation ε_{o1}. This is dependent upon the tensile stress (fineness related tensile force) R_{T_g} which appears in the fibre at the glass transition temperature T_g (for PA 6 nearly 50 °C, for PET nearly 80 °C). For temperatures $< T_g$ the fibre is "ready", this means Tt_s is reached and on the following take-up way the fibre will not be further elongated plastically.

c) R_{T_g} is the tensile stress (fineness related tensile force) at the point $< T_g$. Therefore, it is necessary to analyze the tensile force F_{T_g} at this point because it is valid:

$$R_{T_g} = F_{T_g}/Tt_s \tag{4.46}$$

As informed in [280] and [281] F_{T_g} is improved essentially by an air friction component F_{drag} and an acceleration component F_{inert}, in which both of these components have totally different quantitative importance in the classical spinning ($v_s \leq 1200$ m/min) and in the high speed spinning ($v_s \geq 3000$ m/min). With completing this it should be remarked, that in the classical spinning process the rheological initial force F_{rheo} should be taken into consideration.

d) The air friction force F_{drag} is dependent upon the throughput through the spinneret Q_s, the spinning velocity v_s and the distance between the spinneret and the point at which the fibre reaches the glass transition temperature T_g. This spinneret distance l_{T_g} is essentially dependent upon the throughput through the spinneret Q_s, the spinneret temperature T_s and the cooling conditions (surrounding air velocity, surrounding air temperature and surrounding air humidity).

e) The acceleration force F_{inert} is dependent upon the spinning velocity v_s as well as upon the throughput through the spinneret Q_s.

The verbally described dependences are summarised as shown in the technological scheme Fig. 4.8 and the cause-effect-scheme Fig. 4.9.

Looking at Fig. 4.9 it is evident that the fibre fineness Tt_s is one of the two relevant product variables which effects the tensile stress (fineness related tensile force) R_{T_g}. The latter effects the target quantity fibre orientation

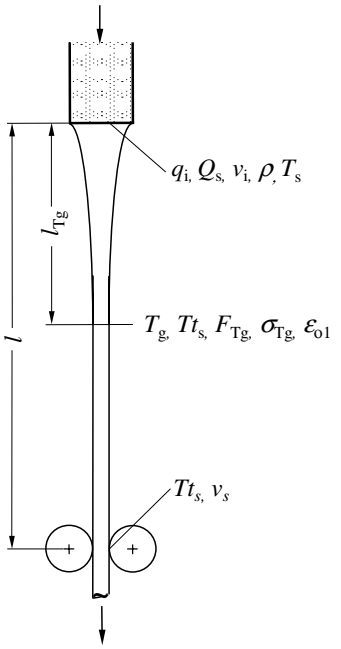

Fig. 4.8. Scheme of fibre formation at the melt spinning of polymers. Solidification point at the glass transition temperature T_g in the distance l_{T_g}

through the elongation orientation ε_{o1}. It would be possible to integrate the whole cause-effect-scheme Fig. 4.2 into Fig. 4.9 for the variable fibre fineness Tt_s. Nevertheless, only the important process variables Q_s and v_s (which directly effect the fineness Tt_s) have been inserted in Fig. 4.9 because these additionally influence the tensile stress (fineness related tensile force) R_{T_g} through the tensile force F_{Tg}.

Estimation to the Disturbance Transfer

In the following it should be attempted to estimate (without detailed derivation) the dynamic disturbance transmission to the fibre orientation ε_{o1} considerating the derived detailed relations from Sect. 4.2.1.

All disturbance quantities which influence Q_s (these are Δv_i, Δq_i and $\Delta\varrho$), effect by means of the ΔTt_s-changes (itself effected by the well-known dynamic transfer equations) also changes of force (ΔR_{T_g})- and with this of orientation elongation ($\Delta\varepsilon_{o1}$)-changes with the same time and frequency behaviour. ΔQ_s-changes additionally cause by means of the F_{T_g}-branch changes ΔR_{T_g} (see Fig. 4.9) in the same manner. The necessarily following change of the stored melt mass in the fibre formation distance with the distance l_{T_g} (which changes too) is decisively for the transfer behaviour of the acceleration force changes as well as for the air friction force changes. The spinning velocity v_s and the distance l_{T_g} are there, on the other hand, the time constant determining quantities for the acceleration and air friction forces. The same

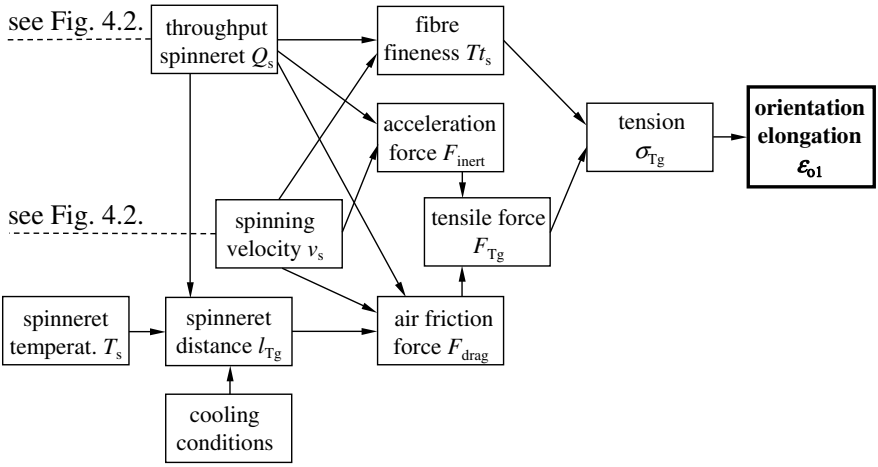

Fig. 4.9. Cause-effect-scheme for the target quantity orientation elongation ε_{o1} at the melt spinning of polymers, especially at the high speed spinning process ($v_s \geq 3000$ m/min)

statement is also valid for the effect of spinning velocity disturbances Δv_s to changes of the orientation elongation $\Delta\varepsilon_{o1}$. The steady state amplification factors are indeed different to estimate for the different disturbance types: Changes of the spinneret throughput ΔQ_s (and its effecting disturbances) effect in each case changes of the fineness Tt_s and also of the tensile force F_{Tg} with equal sign. The effects referred to R_{T_g} and ε_{o1} are comparatively small, because they will be compensated by means of the quotient according to Eq. 4.46. The amplification factor will be small.

Spinning velocity changes Δv_s on the other hand effect changes of the fineness ΔTt_s and also of the tensile force ΔF_{Tg} with unequal sign. The quotient according to Eq. 4.46 for R_{T_g} and its effect to ε_{o1} will be large, and the amplification factor will also be large.

Consequently, spinning velocity changes Δv_s in principle to value are much more influential than spinneret throughput changes ΔQ_s (which are caused for instance by unevenly operating gear pumps, effecting changes of input velocity Δv_i) with view to the generation of structural unevennesses of a melt spun fibre.

The same quantitative data can be authoritative therefore for the velocity of disturbance transmissions to the fibre orientation (and with it to fibre or yarn length with undefined structural properties) than they have been obtained with the dynamic fineness changes.

4.2.3 Complex Proceedings in the Fibre Formation Distance

A *"Specified Differential Equation of a Fibre Formation Distance (simplified)"* has been developed under Sect. 4.2.1. This equation does not consider the first fibre formation range from the spinneret to the solidification point of the melt which characterises the ready fibre state. This actual range of the fibre formation is in principle a range of the highest complex dynamic proceedings even by an undisturbed steady state process. Dynamic change proceedings of all product variables of the fibre formation take place inside this range in a very short time interval. This passage is referred to in Chap. 3, especially to the whole Sect. 3.1 which contains detailed investigations to these complex processes.

4.3 Glass Fibre Spinning; Variable Fibre Fineness

4.3.1 Cause-Effect-Scheme

Another melt spinning material of a totally different source and with different physical and chemical structure is glass. This inorganic fibre material obtained a separate importance for technical-textile applications (especially as a reinforcing fibre material) and (because of its inflammability) for decorative textiles in the last 50 years. Some process dynamic questions for this technological fibre formation process will be discussed in the following sections. Specific further specialities for the methodical practice in the physical analysis of a given technological situation will be explained in more detail later.

The technological scheme of the glass fibre spinning process is shown in Fig. 4.10. [1]

The missing of a spinning pump is evident in comparison with the melt spinning process of polymers (Fig. 4.1). The spinneret is the bottom of a metallic Pt-Rh-oven which is connected serially in the secondary circuit of an electrical heating current transformer. The oven with the spinneret is, in this manner, practically an OHM's heating resistance. The throughput Q_s will be achieved by means of the hydrostatic pressure of the glass melt which stands over the spinneret with the glass level h. A volume feeding spinning pump would not be thinkable here for higher than 1200 °C of the oven temperature. The pressure in front of the spinneret holes p_s is a process

[1] Additionally is to remark, that the so-called two steps process is demonstrated here. Glass marbles (single mass from 10 until 15 g) are fed into the spinneret oven. This is typical for small production or single lab equipments. In large production is to find generally the one step process. The spinneret oven is fed there directly by molten glass mass coming from the glass melt tub and the marble phase is avoided.

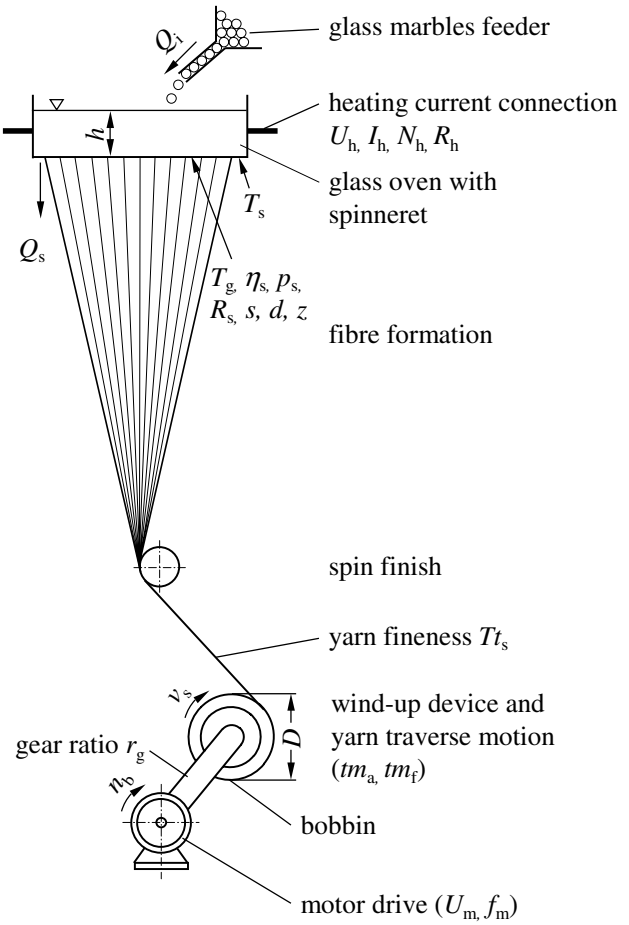

Fig. 4.10. Simplified technological scheme of the glass fibre spinning

variable which directly effects the spinneret throughput Q_s concerning the HAGEN-POISEUILLE-law for viscous melts (in the polymer spinning process, see Fig. 4.2, the pressure p_s was a secondary variable and did not control Q_s and following Tt_s directly!). The valid cause-effect-scheme of the glass spinning process is shown in Fig. 4.11 for the target quantity fineness Tt_s.

These specifics can be learned from Fig. 4.11 in comparison to Fig. 4.2. Another essential specific is that the spinneret temperature T_s (it is the main cause variable for the melt viscosity η_s which effects the flow resistance R_s in the spinneret holes) now directly causes the spinneret throughput Q_s and following the fineness Tt_s.

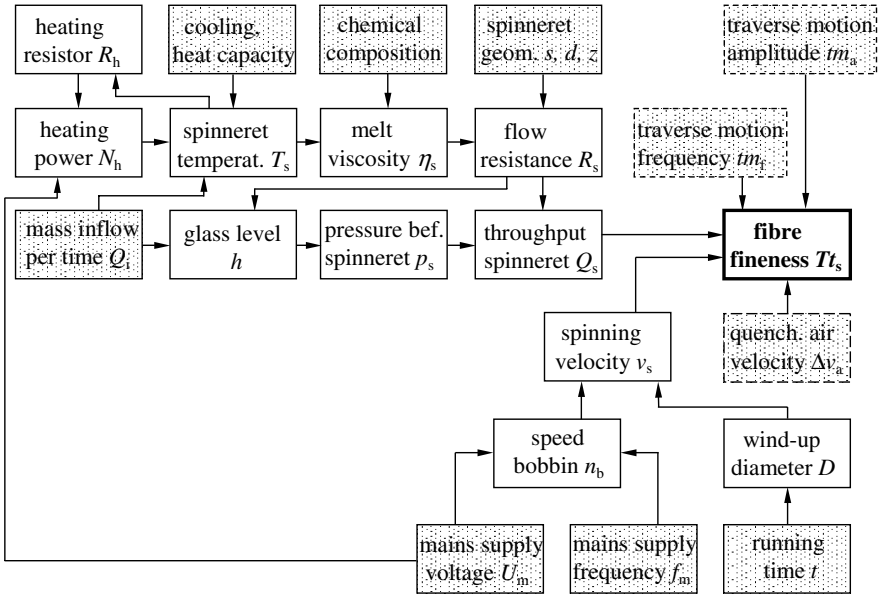

Fig. 4.11. Cause-effect-scheme for the target quantity fibre fineness Tt_s by the glass fibre spinning

The dynamics of the being at hand system has been described in detail in [282, 283] in perspective of possible causes for fibre fineness changes. In the following some few characteristics will be demonstrated which are based upon the general strategy of the technical-physical analysis recommended in Sect. 2.5.1. Specifically it will be clear that each concrete technological situation enforces the consideration or elaboration of new product or process specific a-priori knowledges. An additional product variable at the input of the spinneret oven is the glass mass inflow per time unit Q_i. This variable carries out effects to the glass level h and the spinneret temperature T_s. All other not else named variables of the cause-effect-scheme are explained in Sect. 4.2.1.

4.3.2 Functional Block Diagram

The fibre formation distance possesses, in the glass fibre spinning process, a few other properties than in the polymer spinning in relation to the disturbance transmission. The fibre fineness is actually realised by means of the glass mass inflow per time unit Q_i as well as the spinning velocity v_s. However, the glass fibre is already ready in a distance of 3 to 5 cm below the spinneret holes, because the glass melt does not have a viscous and elastic elongation power. At this point the spinning velocity v_s and the fineness Tt_s are reached. The whole distance between this extremely die near deformation zone until

the take-up bobbin is a pure transport distance in which fineness changes do not take place further. The transmission range of disturbances is reduced to the named short fibre formation distance below the die. This possesses a very small time constant T_c in consequence of the small stored glass mass and the short length from this fibre formation distance. This means further that all disturbances Δv_s and ΔQ_s will be transmitted practically undamped to $\Delta T t_s$. The dynamic properties of the fibre formation distance can be described in the first approximation by means of the steady state model.[2]

Therefore, the single cause-effect relations which produce either ΔQ_s or Δv_s changes must be investigated to the description of the dynamics relating to the product variable fibre fineness. A similar practice would also be necessary for a further complete dynamic "backward" view of an adequate polymer spinning equipment. However, this has been neglected in Sect. 4.2.1, because a spinning pump enforces the spinneret throughput Q_s and the dynamic investigation in the Q_s, as well as in the v_s branch, results in principle in the investigation of the dynamic transmission properties of the electromotoric drives. This will be given now anyway for the lied before glass fibre spinning process in the v_s branch.

The functional block diagram Fig. 4.12 of the cause-effect relations can be designed now on the basis of Fig. 4.11. This supposes partly the mathematical calculation of physical relationships, partly the experimental fixation of the transmission behaviour of single transfer elements. These details are not given here. They are described completely in [282], [283]. As one can see, from the outside imprintable cause quantities to fineness changes $\Delta T t_s$ are possible concerning the dynamic transfer functions G_1 to G_{18} which the transmission effects from changes of the mains supply voltage ΔU_m, changes of the input mass per time unit ΔQ_{i1}, changes of the mains supply frequency Δf_m and changes of the wind-up diameter ΔD, symbolically marked in step response in the single transfer elements of the functional block diagram characterise the transmission behaviour of the concerned element.

A specific of the signal chain is the transfer elements G_2 to G_6 and G_{10} to G_{12} in the present functional block diagram. G_2 to G_6 characterise the (linearised) relationships between a change of a heating voltage ΔU_h and the effected change of the spinneret temperature ΔT_s as a standard example of the electrical heating of an OHM's resistance generally.

G_{10} considers that a change of the glass melt temperature ΔT_g effects a change of the output mass per time unit ΔQ_{s1} as well as (about the transfer

[2] Strictly speaking the transport distance from the end of the deformation zone until the take-up bobbin is the dynamic transmission distance which had to be included in the considerations. This generates however a phase shift only between cause and effect and not a change of the amplitude ratio of cause and effect.

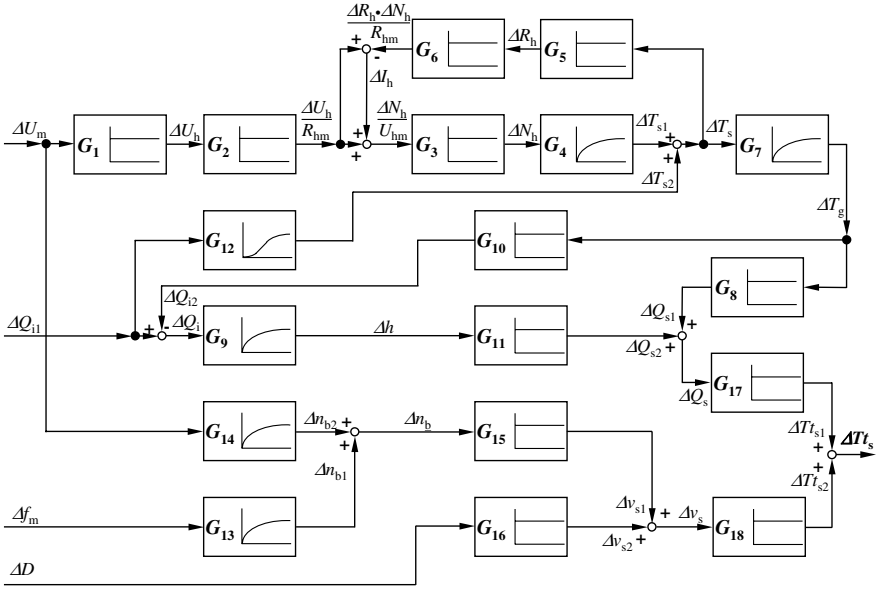

Fig. 4.12. Functional block diagram for the target quantity change fibre fineness ΔTt_s by the glass fibre spinning

element G_9) a change of the glass level Δh. G_{12} considers that a change of the input mass per time unit $\Delta Q_{\mathrm{i}1}$ effects not only a change of the glass level Δh but also a change of the glass melt temperature ΔT_g. G_{10} and G_{12} consider the existing couplings between the temperature and the glass level regime of the spinneret oven.

The most important sizes of the theoretical and experimental investigated glass fibre spinning equipment which characterise the technological regime are collected in Table 4.1, the dynamic transfer functions G_1 to G_{18} are collected in Table 4.2.[3]

Both tables give an impression concerning the physical and technological constants and relationships which are necessary to know for the solution of the given task on the other hand. A better understanding of the following quantitative result interpretations should be obtained herewith.

[3] If it is unambiguously the question of dynamic transfer functions it is often written instead of $G_\mathrm{i}(p)$ shortened G_i. This is used sometimes in the following.

Table 4.1. Compilation of technological and physical constants of the glass fibre melt spinning equipment at the investigated technological operating point

Data to complex	Designation	Symbol	Quantity and dimension
Spinneret oven	number of holes	z	100
	surface of glass melt	A_s	20000 mm^2
	transfer factor of heating transformer	k	$1.023{\cdot}10^{-2}$
	mains supply voltage	U_m	220 V
	heating voltage	U_hm	2.25 V
	heating current	I_hm	2.06 kA
	heating power	N_hm	4.64 kW
	heating (OHMic) resistance of spinneret oven	R_hm	$1.092{\cdot}10^{-3}\Omega$
	spinneret temperature	T_sm	1223 ℃
	glass melt temperature	T_gm	1223 ℃
	glass level	h_m	90 mm
	throughput per spinneret	Q_sm	20 g/min
Winder	speed of bobbin	n_b	2550 min^{-1}
	wind-up diameter	D_m	0.15 m
	gear ratio	r_g	1
	mains supply frequency	f_m	50 Hz
	spinning velocity	v_sm	1200 m/min
	fibre fineness	Tt_sm	16.7 tex
	bobbin formation time	T_bf	10 min
Static amplification factors	transfer element G_4	K_S	100 ℃/kW
	transfer element G_8	$K_{\overline{\mathrm{S}}}$	0.25 $\frac{\mathrm{g}}{\mathrm{min}}$/℃
	transfer element G_9	$K(T_0)$	0.22 $\frac{\mathrm{g}}{\mathrm{min}}$/mm
	transfer element G_{12}	K_K	-1.5 ℃/$\frac{\mathrm{g}}{\mathrm{min}}$
	transfer element G_{13}	K_U	51 min^{-1}/Hz
	transfer element G_{14}	$K_{\overline{\mathrm{U}}}$	2.32 min^{-1}/V
Delay time constants	transfer element G_4	T_H	140 s
	transfer element G_7	$T_{\overline{\mathrm{H}}}$	67 s
	transfer element G_9	T_h	13500 s
	transfer element G_{12}	$T_{\mathrm{K}1}$, $T_{\mathrm{K}2}$	52 s, 386 s
	transfer element G_{13}, G_{14}	T_U	0.9 s
Physical constants	resistance-temperature coefficient of the Pt-Rh-spinneret oven	α_rt	$1.55{\cdot}10^{-4}$/℃
	glass density	ϱ_m	2.5 g/cm^3

Table 4.2. Compilation of the dynamic transfer functions of all functional block diagram elements corresponding to Fig. 4.12

Transfer element G_i	Dynamic transfer function $G_\mathrm{i}(p)$
G_1	$\dfrac{\Delta U_\mathrm{h}}{\Delta U_\mathrm{m}} = k$
G_2	$\dfrac{\Delta U_\mathrm{h}/R_\mathrm{hm}}{\Delta U_\mathrm{h}} = \dfrac{1}{R_\mathrm{hm}}$
G_3	$\dfrac{\Delta N_\mathrm{h}}{\Delta N_\mathrm{h}/U_\mathrm{hm}} = U_\mathrm{hm}$
G_4	$\dfrac{\Delta T_\mathrm{s1}}{\Delta N_\mathrm{h}} = \dfrac{K_\mathrm{S}}{1 + p \cdot T_\mathrm{H}}$
G_5	$\dfrac{\Delta R_\mathrm{h}}{\Delta T_\mathrm{s}} = R_\mathrm{hm} \cdot \alpha_\mathrm{rt}$
G_6	$\dfrac{\Delta R_\mathrm{h} \cdot I_\mathrm{hm}/R_\mathrm{hm}}{\Delta R_\mathrm{h}} = \dfrac{I_\mathrm{hm}}{R_\mathrm{hm}}$
G_7	$\dfrac{\Delta T_\mathrm{g}}{\Delta T_\mathrm{s}} = \dfrac{1}{1 + p \cdot T_{\overline{\mathrm{H}}}}$
G_8	$\dfrac{\Delta Q_\mathrm{s1}}{\Delta T_\mathrm{g}} = K_{\overline{\mathrm{S}}}$
G_9	$\dfrac{\Delta h}{\Delta Q_\mathrm{i}} = \dfrac{1}{K\,(T_0)} \cdot \dfrac{1}{1 + p \cdot T_\mathrm{h}}$
G_{10}	$\dfrac{\Delta Q_\mathrm{i2}}{\Delta T_\mathrm{g}} = K_{\overline{\mathrm{S}}} = G_8$
G_{11}	$\dfrac{\Delta Q_\mathrm{s2}}{\Delta h} = K(T_0)$
G_{12}	$\dfrac{\Delta T_\mathrm{s2}}{\Delta Q_\mathrm{i1}} = \dfrac{K_\mathrm{K}}{(1 + p \cdot T_\mathrm{K1})\,(1 + p \cdot T_\mathrm{K2})}$
G_{13}	$\dfrac{\Delta n_\mathrm{b1}}{\Delta f_\mathrm{m}} = \dfrac{K_\mathrm{U}}{1 + p \cdot T_\mathrm{U}}$
G_{14}	$\dfrac{\Delta n_\mathrm{b2}}{\Delta U_\mathrm{m}} = \dfrac{K_{\overline{\mathrm{U}}}}{1 + p \cdot T_\mathrm{U}}$
G_{15}	$\dfrac{\Delta v_\mathrm{s1}}{\Delta n_\mathrm{b}} = \pi \cdot D_\mathrm{m} \cdot r_\mathrm{g}$
G_{16}	$\dfrac{\Delta v_\mathrm{s2}}{\Delta D} = \pi \cdot n_\mathrm{bm} \cdot r_\mathrm{g}$
G_{17}	$\dfrac{\Delta T t_\mathrm{s1}}{\Delta Q_\mathrm{s}} = \dfrac{1}{v_\mathrm{sm}}$
G_{18}	$\dfrac{\Delta T t_\mathrm{s2}}{\Delta v_\mathrm{s}} = -\dfrac{Q_\mathrm{sm}}{v_\mathrm{sm}^2}$

It means in Table 4.2:

ΔQ_{i1}	change of the input mass per time unit
ΔQ_{s}	change of the output mass per time unit
ΔU_{h}	change of the heating voltage
ΔI_{h}	change of the heating current
ΔN_{h}	change of the heating power
ΔR_{h}	change of the heating (ohmic) resistance
ΔU_{m}	change of the mains supply voltage
Δh	change of the glass level
Δn	change of the speed of bobbin motor
Δf_{m}	change of the mains supply frequency
Δv_{s}	change of the spinning velocity
ΔD	change of the wind-up diameter
ΔT_{s}	change of the spinneret temperature
ΔT_{g}	change of the glass melt temperature
$\Delta T t_{\mathrm{s}}$	change of the fibre fineness

4.3.3 Evaluation and Results

The awaited dynamic changes of the glass fibre fineness $\Delta T t_{\mathrm{s}}$ can be calculated now on the basis of Fig. 4.12 and the relationships which are given in Tables 4.1 and 4.2. The time transient function as well as the complex frequency response can be used. However, the dynamic transfer functions should be preferred to the calculation because a handling, as of items and factors, on the basis of the functional block diagram is possible. The fineness change $\Delta T t_{\mathrm{s2}}$ caused by a change of the mains supply frequency Δf_{m} through the drive of the wind-up bobbin is to be calculated simply for instance by means of the multiplication of the dynamic transfer functions in the cause-effect-chain from Δf_{m} to $\Delta T t_{\mathrm{s2}}$, also

$$\frac{\Delta T t_{\mathrm{s2}}}{\Delta f_{\mathrm{m}}} = G_{13} \cdot G_{15} \cdot G_{18} = -\frac{\pi \cdot K_{\mathrm{U}} \cdot D_{\mathrm{m}} \cdot r_{\mathrm{g}} \cdot Q_{\mathrm{sm}}}{v_{\mathrm{sm}}^2 (1 + p \cdot T_{\mathrm{U}})} \tag{4.47}$$

All interesting total transfer equations can be built up step-like if the following basic rule is considered: Each output size of a transfer element in the functional block diagram is equal to the product of its input size and transfer function of the concerned transfer element, also for instance $\Delta Q_{\mathrm{s1}} = \Delta T_{\mathrm{g}} \cdot G_8$ or $\Delta h = \Delta Q_{\mathrm{i}} \cdot G_9$. This rule is also valid, if single process variables are held constant by means of an additional automatic control. Their changes in size would be then zero (ideal imagination). The following single elements in the functional block diagram would also be assumed to be zero when starting from this points, because their input sizes are missing. If T_{s} were to be controlled, for instance, then ΔT_{s} would be zero in the ideal case and the transfer elements G_7 and G_8 would be inoperative in practice. This would mean that

changes ΔQ_{s1} could not exist anymore and fineness changes could only be induced by means of glass level changes or changes of the wind-up diameter or changes of the speed of the bobbin motor.

Nine different disturbance transfer functions G_{z1} to G_{z9} of the fibre fineness are presented in Table 4.3 which have been calculated on the basis of the dynamic transfer functions G_1 to G_{18} for 9 different disturbance variants. These can be analysed quantitatively after inputting the equation expressions for G_1 until G_{18} given in Table 4.2. The last and further disturbance transfer functions of other process variables (for instance glass level or spinneret temperature) and all resulting amplitude frequency responses, phase frequency responses and step response can be found by the interested reader in [282], [283].

Table 4.3. Compilation of the dynamic disturbance transfer functions of the fibre fineness at the glass fibre spinning

Cause variable disturb.	Additionally const. held variable	Disturbance transfer function $G_{zi}(p)$
ΔU_m	not one	$G_{z1}(p) = \frac{\Delta T t_s}{\Delta U_m} = \frac{2G_1G_2G_3G_4G_7G_{17}\,(G_8 - G_9G_{10}G_{11})}{1 + G_3G_4G_5G_6} + G_{14}G_{15}G_{18}$
ΔU_m	n_b	$G_{z2}(p) = \frac{\Delta T t_s}{\Delta U_m} = \frac{2G_1G_2G_3G_4G_7G_{17}\,(G_8 - G_9G_{10}G_{11})}{1 + G_3G_4G_5G_6}$
ΔU_m	n_b and h	$G_{z3}(p) = \frac{\Delta T t_s}{\Delta U_m} = \frac{2G_1G_2G_3G_4G_7G_{17}}{1 + G_3G_4G_5G_6 - G_7G_{10}G_{12}}$
ΔU_m	h	$G_{z4}(p) = \frac{\Delta T t_s}{\Delta U_m} = \frac{2G_1G_2G_3G_4G_7G_{17}}{1 + G_3G_4G_5G_6 - G_7G_{10}G_{12}} + G_{14}G_{15}G_{18}$
ΔQ_{i1}	not one	$G_{z5}(p) = \frac{T t_s}{\Delta Q_{i1}} = \frac{G_7G_{12}G_{17}\,(G_8 - G_9G_{10}G_{11})}{1 + G_3G_4G_5G_6} + G_9G_{11}G_{17}$
ΔQ_{i1}	T_s	$G_{z6}(p) = \frac{T t_s}{\Delta Q_{i1}} = G_9G_{11}G_{17}$
ΔU_m	T_s	$G_{z7}(p) = \frac{T t_s}{\Delta U_m} = G_{14}G_{15}G_{18}$
Δf_m	not one	$G_{z8}(p) = \frac{T t_s}{\Delta f_m} = G_{13}G_{15}G_{18}$
ΔD	not one	$G_{z9}(p) = \frac{T t_s}{\Delta D} = G_{16}G_{18}$

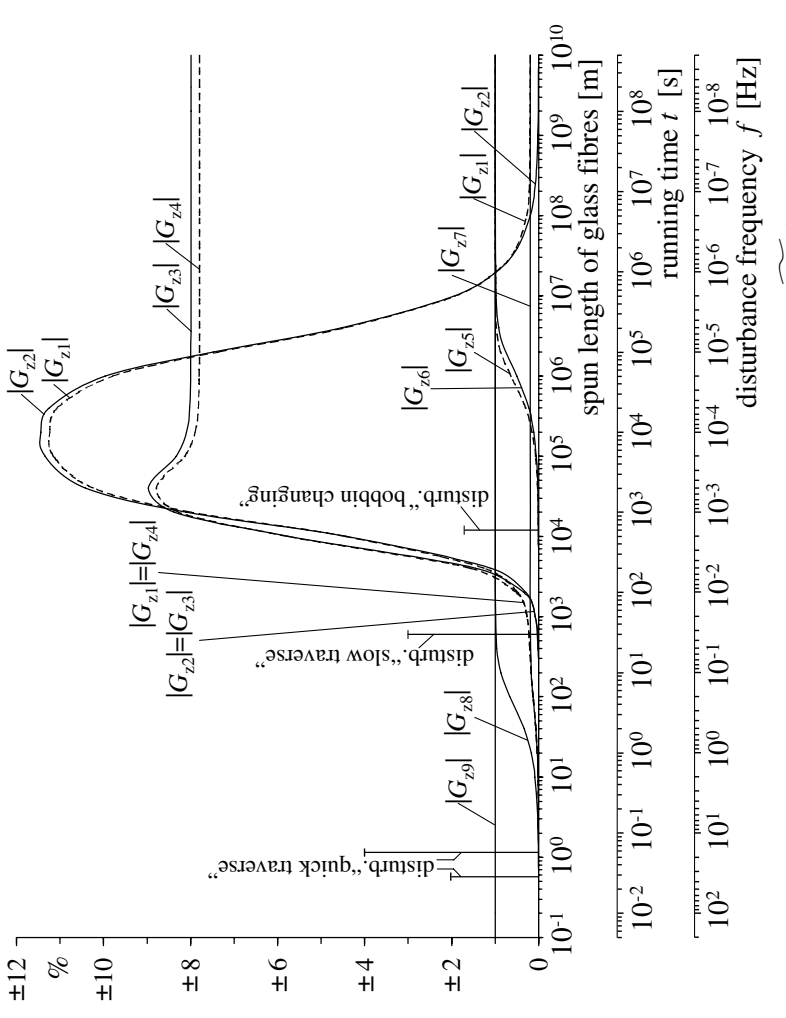

Fig. 4.13. Amplitude frequency responses of percentage fineness changes $(\widetilde{\Delta T t_s}/T t_{sm})100$ by means of changes of different disturbance quantities of 1% by the glass fibre spinning, v_{sm}=1200 m/min

The overview representation Fig. 4.13 is only a demonstration of amplitude frequency responses of the fineness $|G_{z1}(jf)|$ to $|G_{z9}(jf)|$, shortened $|G_{z1}|$ to $|G_{z9}|$.

The oscillations percent of the fineness are drawn on the ordinate which would appear at a one percent sinusoidal disturbance of $\widetilde{\Delta U_m}$, $\widetilde{\Delta Q_{i1}}$, $\widetilde{\Delta f_m}$ or $\widetilde{\Delta D}$ appropriately of the selected disturbance variant. Three interacting measurements are drawn on the abscissa (valid for the special numerical example according to Table 4.1). The first abscissa measurement presents the meter yarn spun from the start time point, the second presents the running time according to the applied spinning velocity, the third the disturbance frequency. The latter is also strongly connected with both of the first measurements. The assertion of Fig. 4.13 should be explained by use of an example.

Assertion of the amplitude frequency response $|G_{z2}|$: Disturbance $\widetilde{\Delta U_m}$ with constant speed of the bobbin motor ($\widetilde{\Delta n_b} = 0$). The mains supply voltage shall oscillate ±1% with a determined frequency sinusoidal around its steady state value of 220 V. If the frequency of the disturbance is very small then the glass level can change quickly enough and the change $\widetilde{\Delta Q_s}$ (caused by $\widetilde{\Delta T_s}$ respectively $\widetilde{\Delta T_g}$) can be compensated. If the frequency of the distrubance increases then $\widetilde{\Delta h}$ cannot follow $\widetilde{\Delta T_s}$ respectively $\widetilde{\Delta T_g}$ quickly enough and a $\widetilde{\Delta T t_s}$ appears starting with small amplitude values. This increases more and more with an increasing f. The amplitude curve stands out against the abscissa and goes to its maximum. This is reached by a disturbance frequency which is identical to the resonance frequency of the system. In this range an oscillation of $\widetilde{\Delta U_m} = \pm\ 1\%$ effects an oscillation of $\widetilde{\Delta T t_s} = \pm\ 10.8\%$. If f increases furthermore then T_g cannot follow quickly enough (involved by the heat inertia of the system) and the amplitudes $\widetilde{\Delta T t_s}$ will again be smaller and smaller. The amplitude frequency response again asymptotically approaches the abscissa.

In the first abscissa measurement it is readable, that the mains supply voltage oscillations in the named critical frequency range operates to the fineness in a length range of 10^3 until $5 \cdot 10^7$ m yarn. This increase is therefore precarious, because the $\widetilde{\Delta U_h}$ (caused by $\widetilde{\Delta U_m}$) can be throughout ± 5% (in a non-automatic controlled process). Fineness oscillations of ± 54% would be the result! The conclusion of the dynamic analysis is that the process must be stabilised by means of an automatic control. However, $\widetilde{\Delta T t_s}$ inside of a yarn length from 10^3 m would not be recordable independently of the quantities of $\widetilde{\Delta U_m}$ respectively $\widetilde{\Delta U_h}$.

The further disturbance inflows can be explained and estimated in an adequate manner using the other curves of the diagram. Four additional single

$\widetilde{\Delta T t_s}$-oscillation parts are drawn in Fig. 4.13 (perpendicular straight lines to the abscissa), which are caused by the yarn winding advance motion and the wind-up diameter changes along a bobbin changing. These four disturbances only exist at four defined frequencies. The length of these straight lines represents the maximum possible fineness oscillations caused by these disturbances.

Figure 4.14 shows the yarn traverse motion element, which is generally used in the glass fibre wind-up process. It consists of a rotating axle with spacious buckled wires at which the yarn slips off. This special traverse motion element generates three distinguished oscillation frequencies. Analytical details shall not be explained here because they are connected to the special traverse motion element with its geometrical and kinematic specifities.

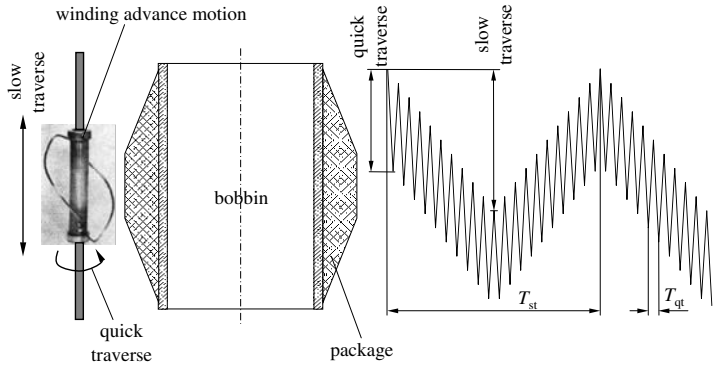

Fig. 4.14. Scheme of the package construction by means of winding advance motion on the glass fibre spinning

The until now given explanations show that practically each disturbance kind in the spinning process will generate changes or oscillations of the fibre fineness. These disturbances of the process variables are the real causes of the fibre or yarn fineness unevenness. This is valid not only for the glass fibre spinning process but for fibre formation processes in general. The dynamical analysis of the whole process allows assertions which cause variables as disturbance sizes are suitable for an appointed target quantity and in which quantity and/or frequency range this will happen.

The reversed question to the conditions for a test proof of appointed disturbance causes in the ready spun yarn will be cleared in Sect. 4.5. We will come back to the summarised presentation of Fig. 4.13 there once more.

4.4 Dynamics of Fibre Formation in the Spun Yarn Spinning Process

4.4.1 Task

The classical technological basic principle to the manufacture of spun staple yarn exists as you may know in different dissolution (beater), parallelisation (roller top card or stationary flat card), and refining (drafting, doubling) process steps of unarranged fibres, mostly pressed in fibre bales, of different length (staple length) to a roving (flyer) which is the input sliver for the last spinning process step, mostly realised by means of a ring frame. The dynamic of the process steps of yarn formation has been investigated and described (only partly or even empirically) in the past frequently under the preparation or realisation view of an automatic control system to influence the fineness unevenness of the produced rovings for the yarn manufacture. Especially the papers are to be mentioned here which present a sufficient and founded dynamic analysis of the automatic controlled process step by means of the time transient function or the dynamic transfer function description [284] to [289].

Two different types of the dynamic system behaviour can be met at the appropriate partial processes: the dead time behaviour [4] and the proportional action with delay [5]. The first is typical for some partial systems of passages in roller top cards and stationary flat cards, the second is for all passages in drafting systems which drafts imprint into the product. The basic equations and some conclusions will be given in the following for both types. Estimations in principle and a further approach to the whole problem should be possible for special tasks.

4.4.2 Dynamic Transfer Behaviour of Carding Engines

Each fibre spinning process pursues the goal to spin yarns with a fineness unevenness as small as possible. Two general strategies can help to reach this goal (besides a further development of the machine technique):
a) by means of a greater number of roving operation passages. This was the only possibility before the invention of automatic controlled drafting systems. The general law underlies this method that a yarn will be more even the more it will be doubled and drafted in the spinning process. However, this is connected as you know with a high expense of machines and (not unimportant)

[4] Changes of a cause variable at the input of a system appears true after a determined time (the dead time) at the output as changes of the effected variable (in the examples of this book it is always a transport time of the treated product). See also Sect. 5.1.3.

[5] To the definition of a proportional action with delay see the first statement of the *"Summarised Evaluation and Conclusions to the Solutions of the Differential Equation"* in Sect. 4.2.1

a lot of working power is necessary.
b) by means of an automatic controlled drafting system in at least one drafting passage in which the draft ratio changes automatically according to the continuously measured fineness changes of the input (open loop control) with or output (closed loop control) slivers. This method allows for drafting and doubling passages to economise in the spinning process plane by an unchanged quality of the ready yarn.

The fineness unevenness of the layed before fibre material (coming from the roller top card or from the stationary flat card as pile, fleece or sliver) is important for both strategies now. At this point, at the latest, the question appears as to the dynamic disturbance transmission on these machines and vice versa to the evenness power for uneven feeded fibre mats, fibre fleeces, fibre flocks and the like.[6]

The dynamic transfer properties of roller top and stationary flat cards have been described previously in the Russian special literature [285] to [287]. The essential ideas are explained in the following which lead to the dynamic transfer function.

Roller Top Card

The technological scheme is shown in Fig. 4.15. Unordered and undissolved fibres will be fed into the machine, picked up from the main drum and conveyed successively to a row of q worker-angle-stripper-pairs i (which $i = 1, 2, 3...q$). In the end the fibres will be processed (dissolved and parallelised) and in each case delivered up to the main drum back. After the run through all work elements the web will be taken up from the main drum and taken off as a sliver. Nevertheless, not all fibres (coming from the main drum) at each work station (consisting of a worker-angle-stripper-pair) go to the concerned worker-angle-stripper-pair but only the K^{th} part $(0 < K < 1)$. The $(1 - K)^{\text{th}}$ part remains on the main drum and will be transported immediately to the next worker-angle-stripper-pair. The, from the worker-angle-stripper-pair picked up, fibres go back to the main drum after the processing or transport time T_{d}. Here also only a part of the fibres (coming from the main drum) will be picked up in fact too at the removal point of the web. This part shall be named K_{a}, whereas the $(1 - K_{\text{a}}^{\text{th}})$ part on the main drum will be mixed to the input of the machine once more after the run of the transport time T_{d2}. The transport time from the flake feeding until the first worker-angle-stripper-pair shall be named T_{d2}. It is assumed, to

[6] At this point the following hint: The dynamic transfer behaviour of the cotton beater (as well-known, directly extending in front of the cotton stationary flat card) has been described fully in [288]. Details must be exempted here. These would exceed the present investigations because these are technologically to far from the fibre formation.

simplify matters, that the coefficient of the fibre distribution K is the same for all worker-angle-stripper-pairs. If this is not the case (in the practice experimental to fix only) different K should be put into the following equations.

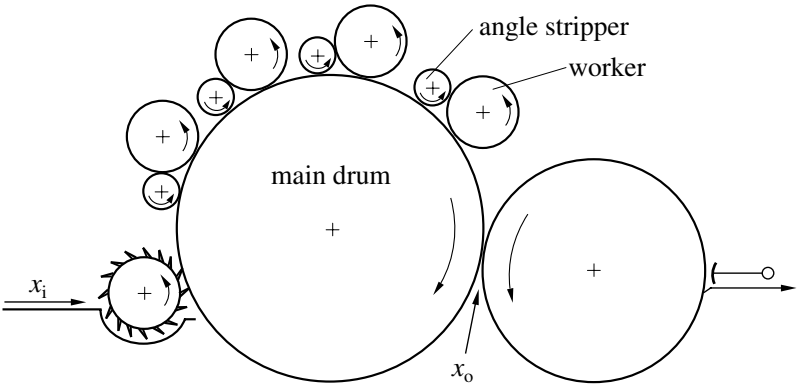

Fig. 4.15. Technological scheme of a roller top card; x_i, x_o input and output fibre mass per time unit

The dynamic transfer function of a roller top card can be developed now by means of the given a-priori knowledge. All quantities are to be taken in equally as changing quantities around the mean averages of an adjusted steady state technological operation point.

The disturbance of the fibre mass Δx_i (caused by uneven flock feed) comes on the main drum at the input of the machine according to Fig. 4.16. This Δx_i will be mixed with the not fully taken up fibre mass Δx_{i1} from the exit of the machine.

The sum passes the dead time element $\exp(-p \cdot T_{d1})$.

$$\Delta x_{i2} = \Delta x_i + \Delta x_{i1} \tag{4.48}$$

This exponential function is the dynamic transfer function of a pure transport or dead time line. The fed fibre mass from the machine entrance appears at the first worker-angle-stripper-pair:

$$\Delta x_1 = \Delta x_{i2} \cdot \exp(-p \cdot T_{d1}) \tag{4.49}$$

The functional block diagram Fig. 4.17 is qualified for the deviation of the dynamic transfer function of a worker-angle-stripper-pair.

The fibre mass Δx_1 (coming from the main drum) and the fibre mass Δx_2 (which is fed back from the processing) will be mixed and the sum Δx will be processed either once more according to the fibre distribution coefficient

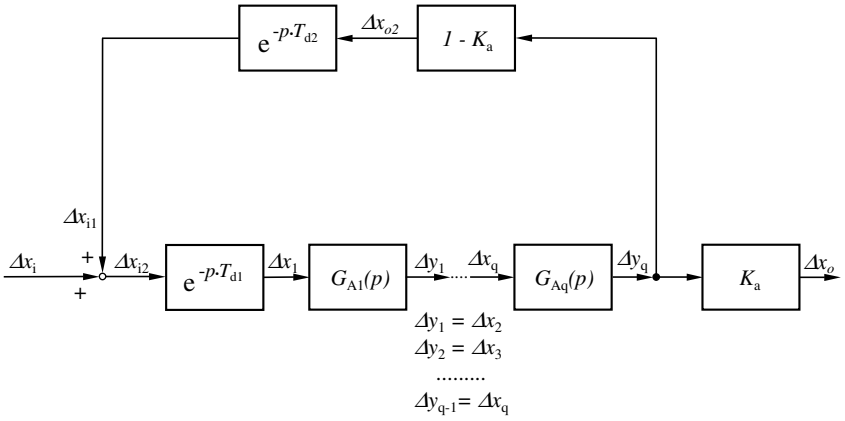

Fig. 4.16. Functional block diagram of the roller top card; Δx_i, Δx_o changes of the input and output fibre mass per time unit

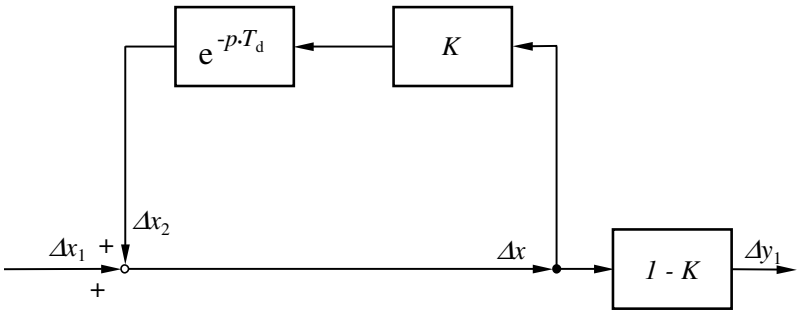

Fig. 4.17. Functional block diagram of the first worker-angle-stripper-pair on the roller top card; Δx_1, Δy_1 changes of the input and output fibre mass per time unit

K (branch with K) or to the main drum transmitted for the next worker-angle-stripper-pair as output fibre mass per time unit Δy_1. The transport time transfer element $\exp(-p \cdot T_\mathrm{d})$ is situated in the branch K. The following equations are readable as:

$$\Delta x = \Delta x_1 + \Delta x_2$$

$$\Delta x_2 = \Delta x \cdot K \cdot \exp(-p \cdot T_{\mathrm{d}1})$$

$$\Delta y_1 = \Delta x \cdot (1 - K)$$

From this it is possible to calculate the dynamic transfer function:

$$G_{\mathrm{W}1}(p) = \frac{\Delta y_1}{\Delta x_1} = \frac{1 - K}{1 - K \cdot \exp(-p \cdot T_\mathrm{d})} \tag{4.50}$$

Because each output Δy_i of a worker-angle-stripper-pair is simultaneously equal the input $\Delta x_{\mathrm{i}+1}$ of the next worker-angle-stripper-pair the dynamic

transfer function of all q worker-angle-stripper-pairs of a roller top card can be written as:

$$G_{\mathrm{W1}}(p) \cdot G_{\mathrm{W2}}(p) \cdots G_{\mathrm{Wq}}(p) = \frac{\Delta y_{\mathrm{q}}}{\Delta x_1} = \left[\frac{1-K}{1-K \cdot \exp(-p \cdot T_{\mathrm{d}})}\right]^q \qquad (4.51)$$

The dynamic transfer function of the whole roller top card can be calculated now considering Eq. 4.51 and the following equations, which are readable from Fig. 4.16 as:

$$\Delta x_{\mathrm{o}} = \Delta y_{\mathrm{q}} \cdot K_{\mathrm{a}}$$

$$\Delta x_{\mathrm{i2}} = \Delta x_{\mathrm{i}} + \Delta x_{\mathrm{i1}}$$

$$\Delta x_{\mathrm{i1}} = \Delta y_{\mathrm{q}} \cdot (1 - K_{\mathrm{a}}) \cdot \exp(-p \cdot T_{\mathrm{d2}})$$

$$\Delta x_1 = \Delta x_{\mathrm{i2}} \cdot \exp(-p \cdot T_{\mathrm{d1}})$$

The final result for the whole roller top card is at last:

$$G_{\mathrm{rc}}(p) = \frac{\Delta x_{\mathrm{o}}}{\Delta x_{\mathrm{i}}} = \frac{K_{\mathrm{a}} \cdot \exp(-p \cdot T_{\mathrm{d1}})}{\left[\dfrac{1-K \cdot \exp(-p \cdot T_{\mathrm{d}})}{1-K}\right]^q - (1-K_{\mathrm{a}}) \cdot \exp[-p(T_{\mathrm{d1}} + T_{\mathrm{d2}})]} \qquad (4.52)$$

The complex frequency response as we know it is obtained when the operator p is substituted by the complex frequency $\mathrm{j}\omega$. Data about the dynamic disturbance transmission properties and about the evenness power of the roller top card are only general and extrapolated from results of possible concrete realised machines. Prerequisites for a quantitative analysis are the knowledge of the fibre distribution coefficients K and K_{a} and the dead times T_{d}, T_{d1} and T_{d2}, which can be appointed only experimentally. Quantitative analyses by means of graphic methods of the vector addition and inversion say [285]:

a) The evenness power of the roller top card is only given for input disturbances of the fed fibre mass per time unit, if the disturbance frequency is large. The cycle duration for a full oscillation must be smaller than the whole transport time of the fibres from the card entrance to its exit. This time can be nearly estimated with $T_{\mathrm{d1}} + q \cdot T_{\mathrm{d}}$.

b) The evenness power of changes, which the conditions under a) actually fulfill, will not take place if the cycle duration of the disturbances is equal or if an integer part multiple of the dead time of a worker-angle-stripper-pair T_{d}. Then namely, the maxima from fibres which come back after the time T_{d} coincide with maxima of the next, after the next and so on disturbance changes.

c) The evenness power is the better the more worker-angle-stripper-pairs are situated on the main drum periphery from the entrance of the card to its exit (trivial assertion) and/or the more uneven these are designed regarding its transport dead time. Because T_d arises from the diameter of the roller and from their speed (that means from their periphery and their periphery velocity) two possibilities of variation are given in principle. This means physically-obviously that resonance conditions should be at another disturbance frequency for each worker-angle-stripper-pair to avoid whole resonance conditions for all disturbance frequencies.

Stationary Flat Card

In comparison to the roller top card with discreet situated working elements on the main drum (worker-angle-stripper-pairs) these melt together to a closed technological unit in form of a flat clothing (Fig. 4.18).

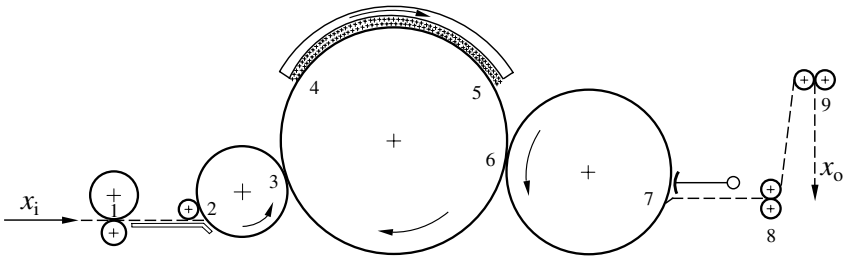

Fig. 4.18. Technological scheme of a stationary flat card; ranges 1 - 2, 7 - 8 and 8 - 9 draft of the web; ranges 2 - 3, 3 - 4, 5 - 6 and 6 - 7 transport of the web; range 4 - 5 treatment of the web

Referring to [287] the following dynamic transfer function has been derived and experimentally confirmed for the stationary flat card:

$$G_{fc}(p) = \frac{\Delta x_o}{\Delta x_i} = \frac{1}{V} \cdot \frac{\exp(-p \cdot T_d)}{1 + (T_{c1} + T_{c2}) \cdot p + T_{c1} T_{c2} \cdot p^2} \tag{4.53}$$

The single symbols mean:

Δx_i, Δx_o changes of the input and output fibre mass

V whole draft of the fibre mass$=\frac{v_{output}}{v_{input}}$
(ranges 1 - 2, 7 - 8, 8 - 9)

T_d sum of all transport times of the fibres
(ranges 2 - 3, 3 - 4, 5 - 6, 6 - 7)

T_{c1}, T_{c2} time constants, describing the dynamic of the fibre redeposition power of the whole flat clothing, which is a fibre mass storage with permanent fibre exchange

With that (Eq. 4.53) the dynamic model of a stationary flat card shows a dead time behaviour (exponential function in the numerator) with delay of second order.

Complex frequency response (4.54), amplitude frequency response (4.55) and phase frequency response (4.56) can be calculated on the basis of Eq. 4.53 as follows:

$$G_{\mathrm{fc}}(\mathrm{j}\omega) = \frac{\widetilde{\Delta x_{\mathrm{o}}}}{\widetilde{\Delta x_{\mathrm{i}}}} \cdot \mathrm{e}^{\mathrm{j}\varphi} = \frac{1}{V} \cdot \frac{\exp(-\mathrm{j}\omega \cdot T_{\mathrm{d}})}{1 + (T_{\mathrm{c1}} + T_{\mathrm{c2}}) \cdot \mathrm{j}\omega + T_{\mathrm{c1}} T_{\mathrm{c2}} \cdot (\mathrm{j}\omega)^2} \tag{4.54}$$

$$|G_{\mathrm{fc}}(\mathrm{j}\omega)| = \left| \frac{\widetilde{\Delta x_{\mathrm{o}}}}{\widetilde{\Delta x_{\mathrm{i}}}} \right| = \frac{1}{V} \left[(1 - T_{\mathrm{c1}} T_{\mathrm{c2}} \omega^2)^2 + \omega^2 (T_{\mathrm{c1}} + T_{\mathrm{c2}})^2 \right]^{-1/2} \tag{4.55}$$

$$\varphi(\omega) = \arctan \left[-\frac{(1 - T_{\mathrm{c1}} T_{\mathrm{c2}} \omega^2) \cdot \sin(\omega T_{\mathrm{d}}) + \omega (T_{\mathrm{c1}} + T_{\mathrm{c2}}) \cdot \cos(\omega T_{\mathrm{d}})}{(1 - T_{\mathrm{c1}} T_{\mathrm{c2}} \omega^2) \cdot \cos(\omega T_{\mathrm{d}}) - \omega (T_{\mathrm{c1}} + T_{\mathrm{c2}}) \cdot \sin(\omega T_{\mathrm{d}})} \right] \tag{4.56}$$

The following equivalent, to the output web of the card referred distances gives both time constants as $T_{\mathrm{c1}} \widehat{=} 2.12$ m, $T_{\mathrm{c2}} \widehat{=} 0.78$ m in [287] for a specific cotton stationary flat card. Hence they follow the time constants after division by the web output velocity v_{o} to:

$$T_{\mathrm{c1}} = 2.12/v_{\mathrm{o}},\ T_{\mathrm{c2}} = 0.78/v_{\mathrm{o}}$$

The times will be derived in the dimension s, if v_{o} is put in the dimension m/s.

The amplitude frequency response according to Eq. 4.55 is shown in Fig. 4.19 and actually not versus the disturbance frequency ω but versus the wavelength λ_{o} in the output web. The used conversion relation can be read as:

$$\omega = 2 \cdot \pi \cdot v_{\mathrm{o}} / \lambda_{\mathrm{o}} \tag{4.57}$$

The awaited evenness effect of the stationary flat card can be estimated from this amplitude frequency response. The normalised to the mean values x_{om} and x_{im} related fluctuation parts $\widetilde{\Delta x_{\mathrm{o}}}$ and $\widetilde{\Delta x_{\mathrm{i}}}$ are represented in the ordinate.

The quotient

$$\frac{\widetilde{\Delta x_{\mathrm{o}}}/x_{\mathrm{om}}}{\widetilde{\Delta x_{\mathrm{i}}}/x_{\mathrm{im}}}$$

is obtained considering the relation

$$V = \frac{v_{\mathrm{om}}}{v_{\mathrm{im}}} = \frac{x_{\mathrm{im}}}{x_{\mathrm{om}}}$$

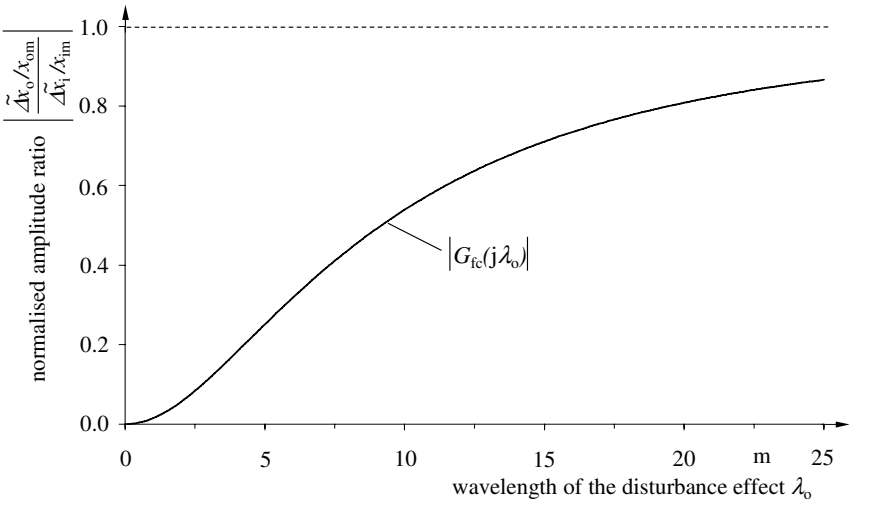

Fig. 4.19. Normalised amplitude frequency response by changes of the output fibre mass per time unit $\widetilde{\Delta x_o}$ caused by changes of the input fibre mass per time unit $\widetilde{\Delta x_i}$ of a stationary flat card

Figure 4.19 shows that a worth-while evenness of input fluctuations $\widetilde{\Delta x_i}$ are only to be awaited to a web length of 5 m, an even good evenness to a web length of 10 m and no worth-while evenness for a web length of more than 15 m. The pertinent wavelength of the disturbance cause in the coming in sliver λ_i of the stationary flat card ($\widetilde{\Delta x_i}$-course) is simple to calculate by using the quotient of λ_o and the draft V:

$$\lambda_i = \lambda_o / V$$

Finally it is to be remarked that the preceding considerations relate only to the fibre mass distribution along the web. Uneven distributions across to the transport direction have been excluded from the considerations because they must be described preferably with other methods. Some hints are represented moreover in [285].

4.4.3 Dynamic Transfer Behaviour of Drafting Zones in Drafting Systems

Specified Differential Equation of a Drafting Zone and its Disturbance Transfer

The drafting or drawing process is the most important processing step for the refinement of the slivers at the roving operation and at the final spinning machines. The dynamic of these processes is not to describe easy by

means of a mathematical model if the statistical discontinuity of the geometrical single fibre properties (above all their length) are to be taken into consideration by the investigations. An impression of the complication (and also unfortunately the unwieldy handling) of a complete model description is shown in [289] and [290]. Nevertheless, it is enough to use the following simplified DEq. and its solutions for the outlet of design lines for automatic control tools of drafting systems or also only for the estimation how the fineness fibre of a sliver will in summary be influenced in such a drafting zone.

On this occasion it is assumed, that

- the fibre number in the sliver cross section at the drafting zone exit is greater than (> 100) and
- the roll setting is $1.5 \cdot l_\mathrm{f} \leq l \leq 2 \cdot l_\mathrm{f}$, in which l_f is the middle staple length of the fibres.

The latter prerequisite means, that neither the drafting forces should increase to high (under limit) nor should "swimming" fibres appear in a greater number which can no longer guarantee the cohesion of the free, not conducted, sliver section.

According to Fig. 4.20 the process and product variables which are necessary for the derivation of the DEq. can be defined in a similar manner as with the drawing zone of the drawing process (Fig. 2.3). They are somewhat the same:

v_i	input velocity
v_o	output velocity
z_i	number of fibres in the cross section of the coming in sliver
z_o	number of fibres in the cross section of the coming out sliver
l	roll setting
l_f	fibre length
Tt_f	fibre fineness
Tt_i	fineness of the coming in sliver $= z_\mathrm{i} \cdot Tt_\mathrm{f}$
Tt_o	fineness of the coming out sliver $= z_\mathrm{o} \cdot Tt_\mathrm{f}$

The dynamic basic Eq. 2.23 for the exchange processes in a mass storage system is similarly valid for the drafting zone. With this it is now possible to immediately describe the dynamic transfer behaviour with the general linearised DEq. 4.7. Single product variables, which apply to the yarn with endless fibres, must be adapted and defined to the present sliver structure. The linearised DEq. which fits the drafting zone of the sliver draft can be defined, if the following variables of Eq. 4.7 are substituted: the middle input cross sectional area q_im and its change Δq_i by the mean number of fibres in the cross sectional area of the input sliver z_im and its change Δz_i. Furthermore the mean density of the fibre material ϱ_m and its change $\Delta\varrho$, here no more consisting of a continuum mass, by the mean fineness of the fibres Tt_fm and

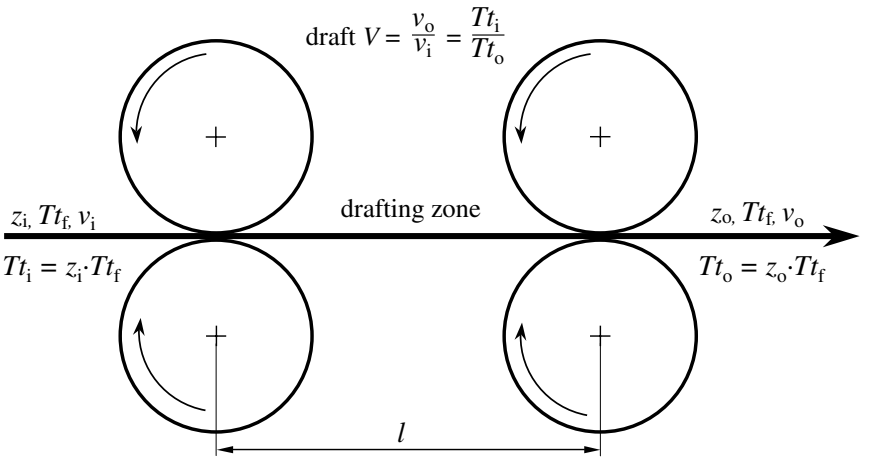

Fig. 4.20. Technological scheme of a one step sliver drafting system

its change ΔTt_f:

$$\begin{aligned}&(v_{om} + p \cdot l_m) \cdot \Delta Tt_o + Tt_{om} \cdot \Delta v_o - v_{im} \cdot Tt_{fm} \cdot \Delta z_i \\ &- z_{im} \cdot Tt_{fm} \cdot \Delta v_i + p \cdot Tt_{om} \cdot \Delta l - z_{im} \cdot v_{im} \cdot \Delta Tt_f = 0\end{aligned} \tag{4.58}$$

The dynamic transfer function of the fineness Tt_o of the yarn at the drafting system output can be given on the basis of Eq. 4.58 which was demonstrated similarly in Sect. 4.2.1. The dynamic functions complex frequency response, amplitude frequency response, phase frequency response and step response for the changes of Δv_o, Δv_i, Δz_i, ΔTt_f or Δl to the effected ΔTt_o-changes can now be derived. Probably, the most interesting dynamic functions (amplitude and step responses) for quantitative estimations are given as follows accordingly to Eqs. 4.13, 4.17, 4.19, 4.23, 4.25, 4.29 and 4.31. The functions for Δl-changes are lost on this occasion because these are not of any interest in drafting systems. The roll setting is assumed as constant and designed as mean value l_m:

disturbance Δv_o *(changes of the output velocity)*
amplitude frequency response

$$|G(j\omega)| = \left| \frac{\widetilde{\Delta Tt_o}}{\widetilde{\Delta v_o}} \right| = (-)\frac{Tt_{om}}{v_{om}} \left[1 + \left(\omega \cdot \frac{l_m}{v_{om}} \right)^2 \right]^{-1/2} \tag{4.59}$$

time transient function (step response)

$$\underline{\Delta Tt_o | \overline{\Delta v_o}} = -\Delta v_o \cdot \frac{Tt_{om}}{v_{om}} \left[1 - \exp\left(-\frac{v_{om}}{l_m} \cdot t \right) \right] \tag{4.60}$$

disturbance Δv_i *(changes of the input velocity)*
amplitude frequency response

$$|G(\mathrm{j}\omega)| = \left| \frac{\widetilde{\Delta T t_\mathrm{o}}}{\widetilde{\Delta v_\mathrm{i}}} \right| = \frac{T t_\mathrm{om}}{v_\mathrm{im}} \left[1 + \left(\omega \cdot \frac{l_\mathrm{m}}{v_\mathrm{om}} \right)^2 \right]^{-1/2} \tag{4.61}$$

time transient function (step response)

$$\underline{\Delta T t_0} | \overline{\Delta v_\mathrm{i}} = \Delta v_\mathrm{i} \cdot \frac{T t_\mathrm{om}}{v_\mathrm{im}} \left[1 - \exp\left(-\frac{v_\mathrm{om}}{l_\mathrm{m}} \cdot t \right) \right] \tag{4.62}$$

disturbance Δz_i *(changes of the number of fibres in the cross section of the coming in sliver)*
amplitude frequency response

$$|G(\mathrm{j}\omega)| = \left| \frac{\widetilde{\Delta T t_\mathrm{o}}}{\widetilde{\Delta z_\mathrm{i}}} \right| = \frac{T t_\mathrm{om}}{z_\mathrm{im}} \left[1 + \left(\omega \cdot \frac{l_\mathrm{m}}{v_\mathrm{om}} \right)^2 \right]^{-1/2} \tag{4.63}$$

time transient function (step response)

$$\underline{\Delta T t_\mathrm{o}} | \overline{\Delta z_\mathrm{i}} = \Delta z_\mathrm{i} \cdot \frac{T t_\mathrm{om}}{z_\mathrm{im}} \left[1 - \exp\left(-\frac{v_\mathrm{om}}{l_\mathrm{m}} \cdot t \right) \right] \tag{4.64}$$

disturbance $\Delta T t_\mathrm{f}$ *(changes of the fibre fineness)*
amplitude frequency response

$$|G(\mathrm{j}\omega)| = \left| \frac{\widetilde{\Delta T t_\mathrm{o}}}{\widetilde{\Delta T t_\mathrm{f}}} \right| = \frac{T t_\mathrm{om}}{T t_\mathrm{fm}} \left[1 + \left(\omega \cdot \frac{l_\mathrm{m}}{v_\mathrm{om}} \right)^2 \right]^{-1/2} \tag{4.65}$$

time transient function (step response)

$$\underline{\Delta T t_\mathrm{o}} | \overline{\Delta T t_\mathrm{f}} = -\Delta T t_\mathrm{f} \cdot \frac{T t_\mathrm{om}}{T t_\mathrm{fm}} \left[1 - \exp\left(-\frac{v_\mathrm{om}}{l_\mathrm{m}} \cdot t \right) \right] \tag{4.66}$$

In all cases it is the question of proportional action with a delay of first order (in Sect. 4.2.1 already described for fibre formation distances) as one can see and Eqs. 4.59 to 4.62 are identical with Eqs. 4.11, 4.13, 4.17 and 4.19. Also the phase frequency responses (here not given once more) are identically with the previously given Eqs. 4.12, 4.18, 4.24 and 4.30 for the appropriate disturbances. This result means, that the normalised complex frequency responses of Fig. 4.4, the normalised amplitude and phase frequency responses of Fig. 4.5 and the normalised step response of the Fig. 4.6 are valid for the estimating of the dynamic behaviour and its graphic presentation of a sliver drafting zone in the same manner. Only the following equivalent relations are to be considered: Δq_i, q_im of the polymer fibre formation correspond to

Δz_i, z_im of the sliver drafting zone and $\Delta\varrho$, ϱ_m of the polymer fibre formation correspond to ΔTt_f, Tt_fm of the sliver drafting zone. On the other hand, Δv_o, v_om, Δv_i, v_im and Δl, z_m are fully identical for both different process steps of the fibre, respectively, yarn formation. The discussion in Sect. 4.2.1 is also consequently valid for the disturbance transmission of drafting zones in drafting systems according to the fineness of the outrunning drafted yarn. An additional hint: The disturbance sizes ΔTt_f and, of even greater importance, Δz_i characterise of course fineness disturbances of the inrunning sliver ΔTt_i whose evenness power chances can be estimated specifically through means of the appropriate (homogeneously constructed) amplitude frequency responses 4.63 and/or 4.65. A good evenness power effect through means of an increased system time constant $T_\mathrm{c} = l_\mathrm{m}/v_\mathrm{om}$ is indeed limited at a sliver drafting system, because the distance of the drafting zone l_m cannot be selected (dependent on the staple length of the single fibres) as large as one would wish. The general observable smaller fineness fibre of long staple spun yarns compared to short staple spun yarns is to be found objectively through the viewpoint of the dynamic system. Because, longer staples enforce imperatively longer roll settings with greater time constants T_c (and smaller critical frequencies f_c) which are more effectively dampening for disturbances.

Disturbance Transfer of a Drafting System with Two Successive Drafting Zones

Disturbance Δz_i (changes of the fibre number in the input sliver). Sliver drafting systems are often created in multi stages. It is the question of how disturbances will be transmitted from the input to the different stages and how these appear finally on the output. A drafting system with two successive drafting zones according to Fig. 4.21 will be investigated in the following.

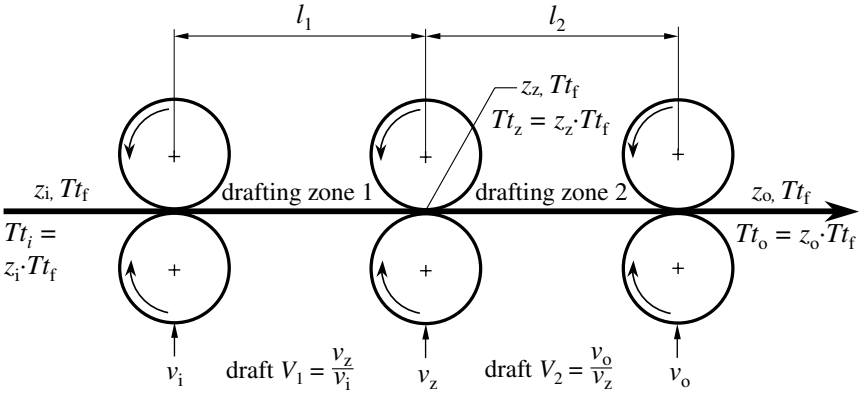

Fig. 4.21. Technological scheme of a two steps sliver drafting system

A sliver with the fineness Tt_i will be drafted to the fineness Tt_o along the drafting zones 1 and 2. The whole draft results as one knows to $V_1 \cdot V_2$ and the steady state equation is valid:

$$Tt_0 = \frac{Tt_\mathrm{i}}{V_1 \cdot V_2} = Tt_\mathrm{i} \cdot \frac{v_\mathrm{i}}{v_\mathrm{o}} \tag{4.67}$$

disturbance variant 1

There should exist a fineness disturbance at the input as a change of the fibre number in the input sliver cross sectional area Δz_i. How will ΔTt_o appear at the output of the second drafting zone? The following process and product variables are to be defined additionally compared with the previous section: The dynamic transfer functions for the drafting zones 1 and 2 must

v_z	velocity of the middle drafting godet pair (output velocity of the drafting zone 1 and simultaneously input velocity of the drafting zone 2)
z_z	number of fibres in the cross section of the coming out sliver from the drafting zone 1 and simultaneously of the coming in sliver into the drafting zone 2
l_1	length of the drafting zone 1
l_2	length of the drafting zone 2
Tt_z	sliver fineness at the output of the drafting zone 1 and the input of the drafting zone 2 $= z_\mathrm{z} \cdot Tt_\mathrm{f}$

be derived at first from the dynamic basic Eq. 4.58 which correspond to the question.
This is for the drafting zone 1:

$$G_1(p) = \frac{\Delta Tt_\mathrm{z}}{\Delta z_\mathrm{i}} = \frac{Tt_\mathrm{zm}}{z_\mathrm{im}} \cdot \frac{1}{1 + p \cdot \dfrac{l_\mathrm{1m}}{v_\mathrm{zm}}} \tag{4.68}$$

One considers that the output fineness of the drafting zone 1 is Tt_z and not Tt_o which at first appears at the output of the drafting zone 2. Therefore, the quantities ΔTt_o and Tt_om have been substituted by the quantities ΔTt_z and Tt_zm in Eq. 4.58 before the Eq. 4.68 has been derived.
The drafting zone 2 is valid as:

$$G_2(p) = \frac{\Delta Tt_\mathrm{o}}{\Delta z_\mathrm{z}} = \frac{Tt_\mathrm{om}}{z_\mathrm{zm}} \cdot \frac{1}{1 + p \cdot \dfrac{l_\mathrm{2m}}{v_\mathrm{om}}} \tag{4.69}$$

If the fineness of the fibres Tt_fm is also constantly valid as
$Tt_\mathrm{zm} = z_\mathrm{zm} \cdot Tt_\mathrm{fm}$ and $\Delta Tt_\mathrm{z} = \Delta z_\mathrm{z} \cdot Tt_\mathrm{fm}$
Therefore Eq. 4.68 is also to be written as:

$$G_1(p) = \frac{\Delta z_z \cdot Tt_{fm}}{\Delta z_i} = \frac{z_{zm} \cdot Tt_{fm}}{z_{im}} \cdot \frac{1}{1 + p \cdot \dfrac{l_{1m}}{v_{zm}}} \tag{4.70}$$

The dynamic transfer function of the successive systems results from the product of the transfer functions of the single systems. If one applies this law to Eqs. 4.69 and 4.70 the following will be obtained for the two steps drafting system:

$$G_D(p) = G_1(p) \cdot G_2(p) = \frac{\Delta Tt_o}{\Delta z_i} = \frac{Tt_{om}}{z_{im}} \cdot \frac{1}{\left(1 + p \cdot \dfrac{l_{1m}}{v_{zm}}\right)\left(1 + p \cdot \dfrac{l_{2m}}{v_{om}}\right)} \tag{4.71}$$

The *complex frequency response* follows from this:

$$G_D(j\omega) = \frac{\widetilde{\Delta Tt_o}}{\widetilde{\Delta z_i}} \cdot e^{j\varphi} = \frac{Tt_{om}}{z_{im}} \cdot \frac{1}{\left(1 + j\omega \cdot \dfrac{l_{1m}}{v_{zm}}\right)\left(1 + j\omega \cdot \dfrac{l_{2m}}{v_{om}}\right)} \tag{4.72}$$

Equation 4.72 can be split into the *amplitude frequency response*

$$|G_D(j\omega)| = \left| \frac{\widetilde{\Delta Tt_o}}{\widetilde{\Delta z_i}} \right| = \frac{Tt_{om}}{z_{im}} \cdot \frac{\sqrt{\left[1 - \omega^2 \cdot \dfrac{l_{1m} \cdot l_{2m}}{v_{zm} \cdot v_{om}}\right]^2 + \omega^2 \left[\dfrac{l_{1m}}{v_{zm}} + \dfrac{l_{2m}}{v_{om}}\right]^2}}{\left[1 + \left(\omega \cdot \dfrac{l_{1m}}{v_{zm}}\right)^2\right]\left[1 + \left(\omega \cdot \dfrac{l_{2m}}{v_{om}}\right)^2\right]} \tag{4.73}$$

and into the *phase frequency response*

$$\varphi(\omega) = \arctan\left[-\omega \cdot \frac{\dfrac{l_{1m}}{v_{zm}} + \dfrac{l_{2m}}{v_{om}}}{1 - \omega^2 \cdot \dfrac{l_{1m} \cdot l_{2m}}{v_{zm} \cdot v_{om}}}\right] \tag{4.74}$$

Now the *time transient function* to be calculated from Eq. 4.71 is analogous to Eq. 2.41:

$$\begin{aligned} \underline{\Delta Tt_o}|\overline{\Delta z_i} = \Delta z_i \cdot \frac{Tt_{om}}{z_{im}} \left[1 - \frac{v_{om} \cdot l_{1m}}{v_{om} \cdot l_{1m} - v_{zm} \cdot l_{2m}} \cdot \exp\left(-\frac{v_{zm}}{l_{1m}} \cdot t\right)\right] \\ -\Delta z_i \cdot \frac{Tt_{om}}{z_{im}} \cdot \frac{v_{zm} \cdot l_{2m}}{v_{zm} \cdot l_{2m} - v_{om} \cdot l_{1m}} \cdot \exp\left(-\frac{v_{om}}{l_{2m}} \cdot t\right) \end{aligned} \tag{4.75}$$

Equations 4.72 to 4.75 do not mediate a clear assertion about the dynamic properties of the two steps drafting system without of course an appropriate quantitative analysis. The dynamic transfer properties should be demonstrated using a numerical example. It should be assumed:

v_{im} = 1 m/min
v_{om} = 36 m/min
v_{zm} = 1.5 m/min (V_1=1.5; V_2=24) or 6 m/min (V_1=6; V_2=6)
Tt_{im} = 1000 tex
z_{im} = 3600
Tt_{fm} = 0.28 tex
Tt_{om} = 27.8 tex
z_{om} = 100
$l_{2\mathrm{m}}$ = 45 mm
$l_{1\mathrm{m}}$ = 50 mm or 40 mm

The disturbance should be step-like or sinusoidal $\Delta z_{\mathrm{i}} = 180$ respectively $\widetilde{\Delta z_{\mathrm{i}}} = \pm 180$.

The time constants T_{cd1} and T_{cd2} and the critical frequencies f_{c1} and f_{c2} of the drafting zones 1 and 2 according to Eqs. 2.47 and 2.49 are:

		Drafting zone 1		Drafting zone 2	
$l_{1\mathrm{m}}$ [mm]	v_{zm} [m/min]	T_{cd1} [s]	f_{c1} [Hz]	T_{cd2} [s]	f_{c2} [Hz]
50	1.5	2.00	0.080	0.075	2.12
50	6	0.50	0.318	0.075	2.12
40	1.5	1.60	0.099	0.075	2.12
40	6	0.40	0.398	0.075	2.12

The normalised presentations of the complex frequency response, the amplitude frequency response and the step response are similarly valid if disturbances Δz_{i}, ΔTt_{f} or also Δv_{i} appear at the input. The result interpretation is qualitatively and quantitatively the same for these product and process variables regarding the effect to the output fineness ΔTt_{o}. The phase frequency response is of course similarly valid for all three disturbances.

The transfer locus of the complex frequency response, the amplitude frequency response and the phase frequency response of a two steps sliver drafting system are shown in Figs. 4.22, 4.23 and 4.24. The amplitude and phase diagrams include in each case through agreement two additional curves (drawn dotted) of a one step drafting zone. The appropriate step response is shown in Fig. 4.25.

The following statements can be taken from the diagrams:

a) The evenness power effect is more exact the more unsymmetrical the whole draft is divided between the drafting zones 1 and 2. And indeed, the

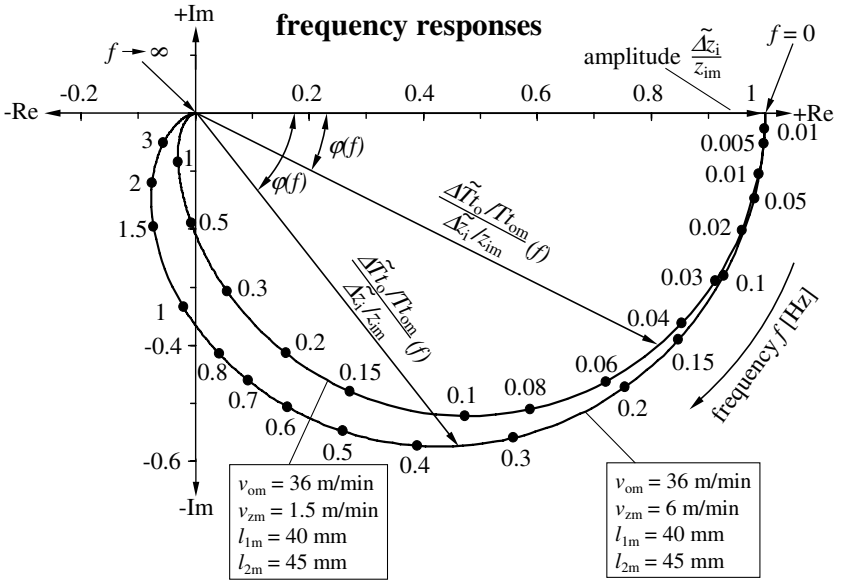

Fig. 4.22. Transfer locuses of the normalised complex frequency responses of fineness changes $\widetilde{\Delta Tt_o}$ in the coming out sliver caused by changes of the number of fibres in the coming in sliver $\widetilde{\Delta z_i}$ at a two steps sliver drafting system

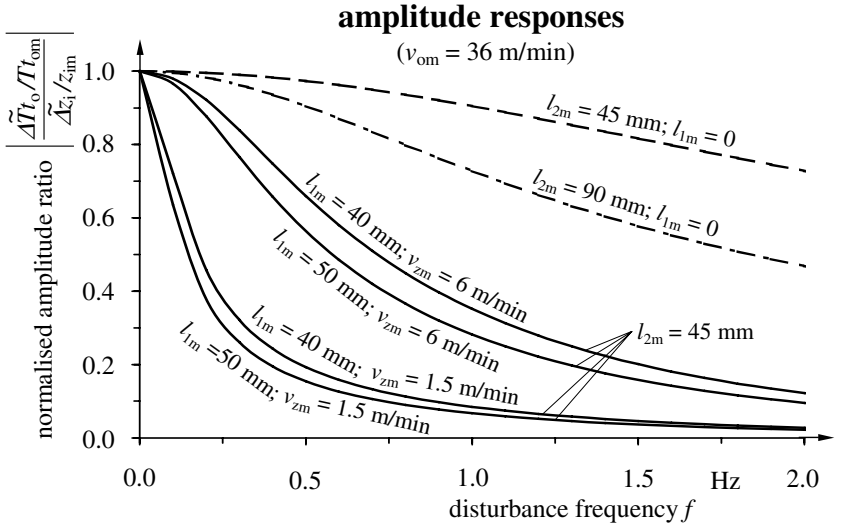

Fig. 4.23. Normalised amplitude frequency responses of fineness changes $\widetilde{\Delta Tt_o}$ in the coming out sliver caused by changes of the number of fibres in the coming in sliver $\widetilde{\Delta z_i}$ at a two steps sliver drafting system

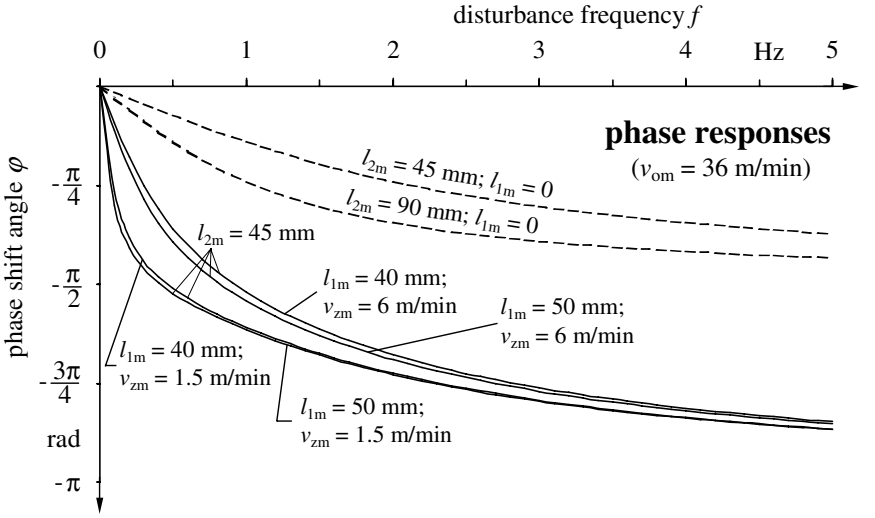

Fig. 4.24. Normalised phase frequency responses of fineness changes $\widetilde{\Delta T t_o}$ in the coming out sliver caused by changes of the number of fibres in the coming in sliver $\widetilde{\Delta z_i}$ at a two steps sliver drafting system

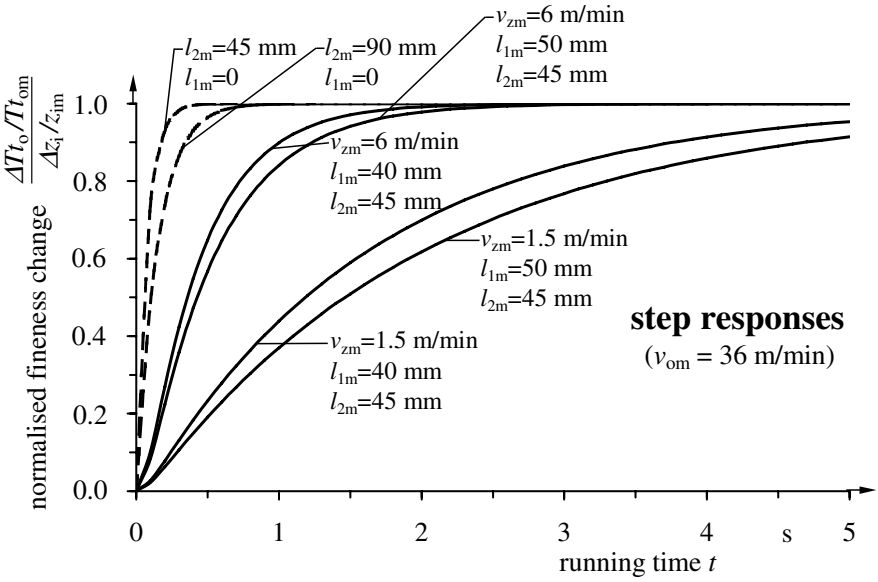

Fig. 4.25. Normalised step response of the fineness changes $\Delta T t_o$ of the coming out sliver caused by changes of the number of fibres in the coming in sliver Δz_i at an one and two steps sliver drafting system

greater part of the draft should be created in the drafting zone 2. This is to be seen by the amplitude frequency response courses which fall down to the abscissa at already clearly smaller disturbance frequencies for $v_z = 1.5$ m/min than for $v_z = 6$ m/min. This tendency can also be seen in the step transfer behaviour. The curves of $v_z = 1.5$ m/min clearly increase more slowly than those for $v_z = 6$ m/min.

b) A change of the first drafting zone length by 10 mm (from a starting point of 40 or 50 mm) does not effect aggravating changes of the dynamic behaviour. The longer drafting zone 1 improves the dampening behaviour for disturbances only insignificantly. A longer drafting zone 2 by same or similar quantities is not practically of influence to the dynamic transmission behaviour (not drawn here because appropriate diagram curves are nearly identical).

c) The comparison with the dropped drawn curves for the one step drafting system (following from the two steps system if l_{1m} is set to zero; compare also Eqs. 4.73 and 4.75 with 4.63 and 4.64) shows that a multi step drafting system (here demonstrated using the two steps system) a more effective evenness power is allowed than a one step drafting system for the fineness of the output sliver in a greater frequency range. In our example the two steps drafting system is able to suppress input disturbances with > 1 Hz to the fineness effectively if the draft is divided skillfully. This would mean for the output sliver in our example that a short periodic unevennesses of sliver length < 60 cm would not appear anymore in a troublesome manner. The same effect would occur for the comparable short one step drafting system only at > 15 Hz, appropriate < 9 m sliver length.

Disturbance Δv_z (velocity changes of the middle drafting roll pair). There should exist step-like or periodic disturbances of the velocity of the middle drafting godet pair v_z. How will ΔTt_o appear at the output of the drafting system?

disturbance variant 2

The mean value of the output fineness Tt_{om} will not change even after longtime disturbances of v_z, because in this case the whole draft does not change steady state. But short time ΔTt_o-effects will appear. These consist of two primary effective transmission processes: Δv_z effects at first a change of the fineness Tt_z at the output of the drafting zone 1, which is simultaneously an input fineness disturbance of the drafting zone 2. Second, Δv_z effects an input velocity disturbance of the drafting zone 2. ΔTt_o consists of the two parts ΔTt_{o1} and ΔTt_{o2} which are consequently to be added according to the superposition law. ΔTt_{o1} describes the disturbance transmission of ΔTt_z to

ΔTt_{o} and ΔTt_{o2} describes the disturbance transmission of Δv_{z} to ΔTt_{o}.

The dynamic transfer behaviour is to be derived from the dynamic transfer functions of the single part drafting zones.

effect of Δv_{z} *to* ΔTt_{z}:

$$G_1(p) = \frac{\Delta Tt_{\mathrm{z}}}{\Delta v_{\mathrm{z}}} = -\frac{Tt_{\mathrm{zm}}}{v_{\mathrm{zm}}} \cdot \frac{1}{1 + p \cdot \dfrac{l_{1\mathrm{m}}}{v_{\mathrm{zm}}}} \tag{4.76}$$

effect of ΔTt_{z} *to* ΔTt_{o1}:

$$G_2(p) = \frac{\Delta Tt_{\mathrm{o1}}}{\Delta Tt_{\mathrm{z}}} = \frac{Tt_{\mathrm{om}}}{Tt_{\mathrm{zm}}} \cdot \frac{1}{1 + p \cdot \dfrac{l_{2\mathrm{m}}}{v_{\mathrm{om}}}} \tag{4.77}$$

effect of Δv_{z} to ΔTt_{o1} = product of Eqs. 4.76 and 4.77:

$$G_3(p) = \frac{\Delta Tt_{\mathrm{o1}}}{\Delta v_{\mathrm{z}}} = -\frac{Tt_{\mathrm{om}}}{v_{\mathrm{zm}}} \cdot \frac{1}{\left(1 + p \cdot \dfrac{l_{1\mathrm{m}}}{v_{\mathrm{zm}}}\right)\left(1 + p \cdot \dfrac{l_{2\mathrm{m}}}{v_{\mathrm{om}}}\right)} \tag{4.78}$$

effect of Δv_{z} *to* ΔTt_{o2}:

$$G_4(p) = \frac{\Delta Tt_{\mathrm{o2}}}{\Delta v_{\mathrm{z}}} = \frac{Tt_{\mathrm{om}}}{v_{\mathrm{zm}}} \cdot \frac{1}{1 + p \cdot \dfrac{l_{2\mathrm{m}}}{v_{\mathrm{om}}}} \tag{4.79}$$

The total ΔTt_{o} is the sum of ΔTt_{o1} and ΔTt_{o2}. The total transfer function $G_{\mathrm{D}}(p)$ is for this disturbance case the sum of $G_3(p)$ and $G_4(p)$ according to Eqs. 4.78 and 4.79:

$$G_{\mathrm{D}}(p) = \frac{\Delta Tt_{\mathrm{o1}}}{\Delta v_{\mathrm{z}}} = \frac{Tt_{\mathrm{om}}}{v_{\mathrm{zm}}} \cdot \frac{p \cdot \dfrac{l_{1\mathrm{m}}}{v_{\mathrm{zm}}}}{\left(1 + p \cdot \dfrac{l_{1\mathrm{m}}}{v_{\mathrm{zm}}}\right)\left(1 + p \cdot \dfrac{l_{2\mathrm{m}}}{v_{\mathrm{om}}}\right)} \tag{4.80}$$

Equation 4.80 shows that a differential action with delay of second order lies before (no permanent fineness shift after a steady state disturbance). It is the starting point for the equations of the frequency, amplitude, phase and step response which can be derived according to the already cited manifold rules of Sect. 2.5.2.

complex frequency response

$$G_{\mathrm{D}}(\mathrm{j}\omega) = \frac{\widetilde{\Delta Tt_{\mathrm{o1}}}}{\widetilde{\Delta v_{\mathrm{z}}}} = \frac{Tt_{\mathrm{om}}}{v_{\mathrm{zm}}} \cdot \frac{\mathrm{j}\omega \cdot \dfrac{l_{1\mathrm{m}}}{v_{\mathrm{zm}}}}{\left(1 + \mathrm{j}\omega \cdot \dfrac{l_{1\mathrm{m}}}{v_{\mathrm{zm}}}\right)\left(1 + \mathrm{j}\omega \cdot \dfrac{l_{2\mathrm{m}}}{v_{\mathrm{om}}}\right)} \tag{4.81}$$

amplitude frequency response

$$|G_{\mathrm{D}}(\mathrm{j}\omega)| = \left| \frac{\widetilde{\Delta T t_{\mathrm{o}}}}{\widetilde{\Delta v_{\mathrm{z}}}} \right| = \frac{T t_{\mathrm{om}}}{v_{\mathrm{zm}}} \cdot \frac{\omega \cdot \frac{l_{1\mathrm{m}}}{v_{\mathrm{zm}}} \sqrt{\left[1 - \omega^2 \cdot \frac{l_{1\mathrm{m}} \cdot l_{2\mathrm{m}}}{v_{\mathrm{zm}} \cdot v_{\mathrm{om}}}\right]^2 + \omega^2 \left[\frac{l_{1\mathrm{m}}}{v_{\mathrm{zm}}} + \frac{l_{2\mathrm{m}}}{v_{\mathrm{om}}}\right]^2}}{\left[1 + \left(\omega \cdot \frac{l_{1\mathrm{m}}}{v_{\mathrm{zm}}}\right)^2\right] \left[1 + \left(\omega \cdot \frac{l_{2\mathrm{m}}}{v_{\mathrm{om}}}\right)^2\right]} \tag{4.82}$$

phase frequency response

$$\varphi(\omega) = \operatorname{arc\,tan} \left[\frac{1 - \omega^2 \cdot \frac{l_{1\mathrm{m}} \cdot l_{2\mathrm{m}}}{v_{\mathrm{zm}} \cdot v_{\mathrm{om}}}}{\omega \left(\frac{l_{1\mathrm{m}}}{v_{\mathrm{zm}}} + \frac{l_{2\mathrm{m}}}{v_{\mathrm{om}}} \right)} \right] \tag{4.83}$$

step response

$$\underline{\Delta T t_{\mathrm{o}}} | \overline{\Delta v_{\mathrm{z}}} = \Delta v_{\mathrm{z}} \cdot \frac{T t_{\mathrm{om}}}{v_{\mathrm{zm}}} \cdot \frac{\exp\left(-\frac{l_{1\mathrm{m}}}{v_{\mathrm{zm}}} \cdot t\right) - \exp\left(-\frac{l_{2\mathrm{m}}}{v_{\mathrm{om}}} \cdot t\right)}{1 - \frac{l_{2\mathrm{m}} \cdot v_{\mathrm{zm}}}{l_{1\mathrm{m}} \cdot v_{\mathrm{om}}}} \tag{4.84}$$

The transfer locus of the frequency, amplitude and phase frequency responses of a two steps sliver drafting system for the disturbance Δv_{z} are shown in Figs. 4.26, 4.27 and 4.28. The step response is shown in Fig. 4.29.

Some statements can also be given here in principle:

a) Extremely short periodic as well as long periodic, fluctuations of the velocity of the middle drafting godet pair also effect the output fineness dampened strength (see amplitude frequency response curves). The range of the maximum disturbance transmission in the example is situated between about 0.5 and 1 Hz. Relative periodic Δv_{z}-changes have nearly the same great $\Delta T t_{\mathrm{o}}$-changes and are actually for strong unsymmetric draft partition ($v_{\mathrm{zm}} = 1.5$ m/min) somewhat greater than for less unsymmetric draft partition ($v_{\mathrm{zm}} = 6$ m/min).

b) This disturbance type Δv_{z} does not cause permanent fineness shifts after a step-like disturbance (see step response). The old fineness mean value $T t_{\mathrm{om}}$ will be reached after a sufficient long time (here > 5 s) also if the disturbance continues. The drafting system further operates with increased

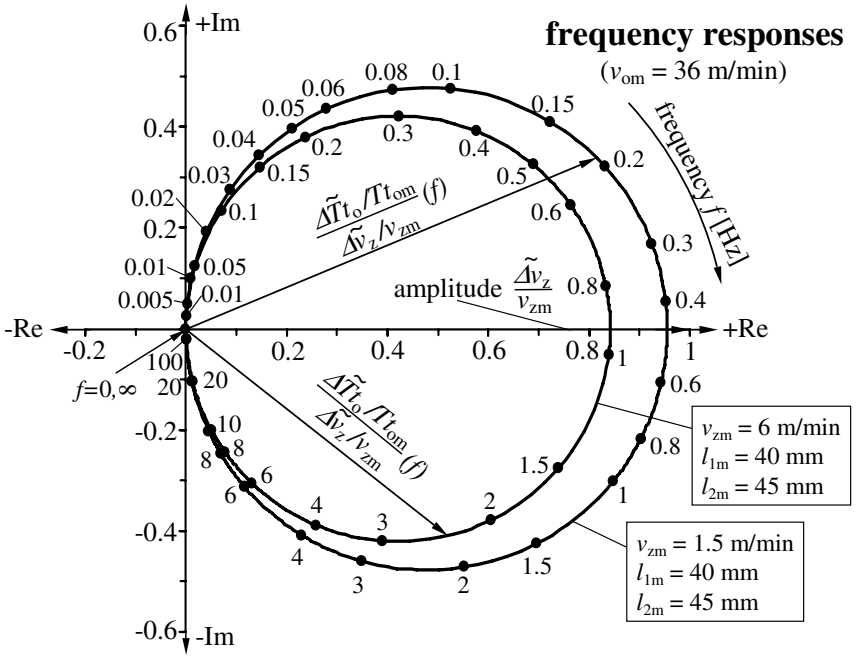

Fig. 4.26. Transfer locuses of the normalised complex frequency responses of fineness changes $\widetilde{\Delta Tt_o}$ in the coming out sliver caused by velocity changes $\widetilde{\Delta v_z}$ of the middle godets at a two steps sliver drafting system

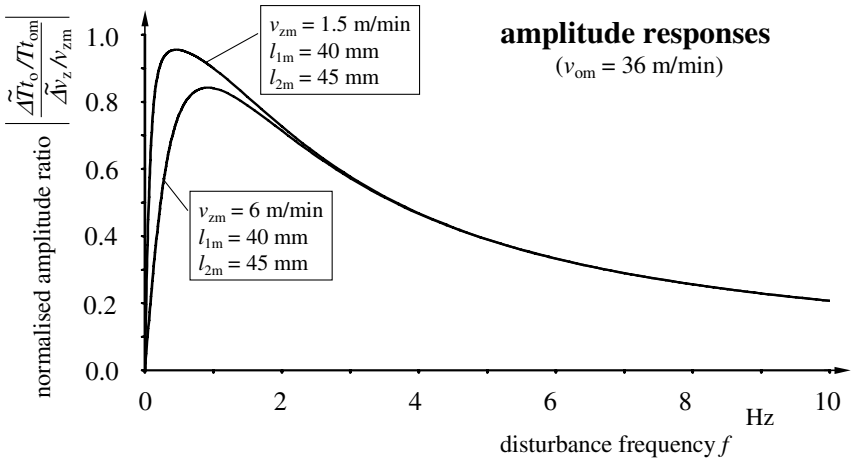

Fig. 4.27. Normalised amplitude frequency responses of fineness changes $\widetilde{\Delta Tt_o}$ in the coming out sliver caused by velocity changes $\widetilde{\Delta v_z}$ of the middle godets at a two steps sliver drafting system

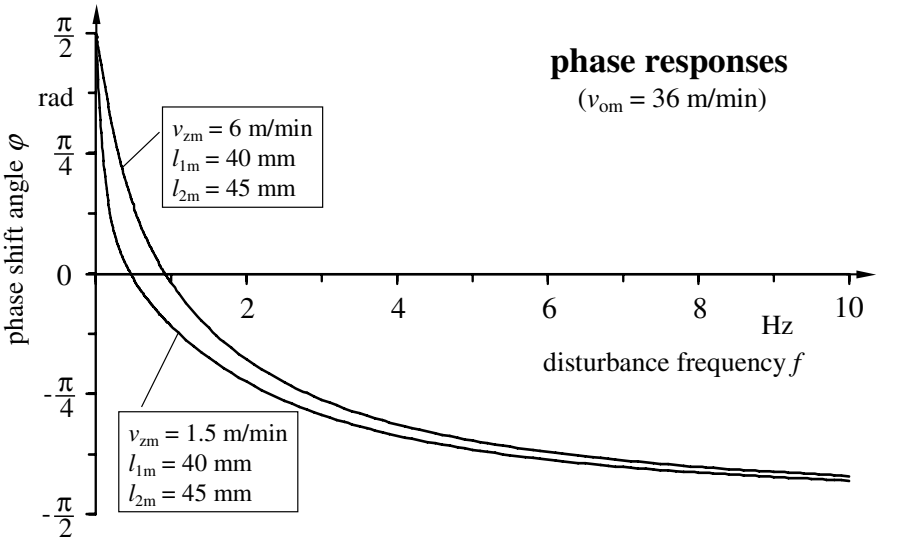

Fig. 4.28. Normalised phase frequency responses of fineness changes $\widetilde{\Delta T t_o}$ in the coming out sliver caused by velocity changes $\widetilde{\Delta v_z}$ of the middle godets at a two steps sliver drafting system

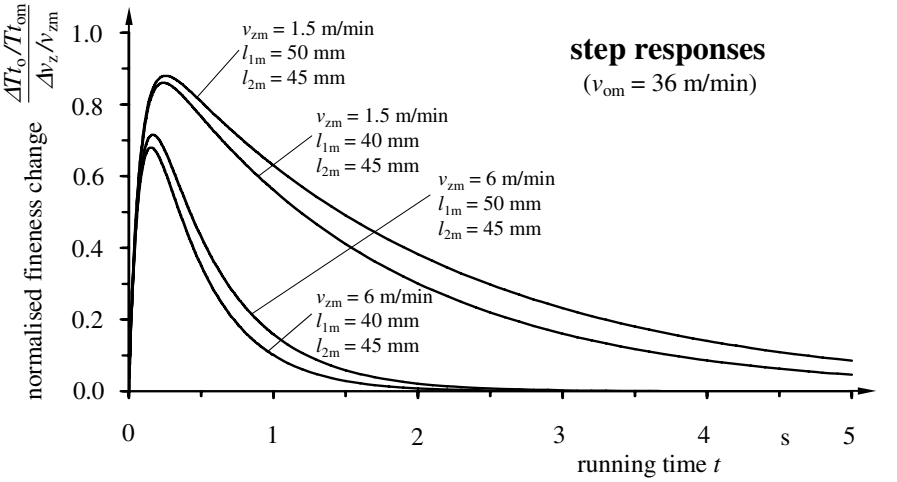

Fig. 4.29. Normalised step responses of the fineness changes $\Delta T t_o$ of the coming out sliver caused by changes of the number of fibres in the coming in sliver Δv_z at a one and two steps sliver drafting system

draft in zone 1 and simultaneously with decreased draft in zone 2 in which the total draft is unchanged. It is also to be observed here that greater short time shifts of the fineness appear if the total draft is chosen unsymmetrically. Length changes of the drafting zone 1 have a smaller influence in which an increase of l_{1m} effects a small increase of the fineness shift.

c) A result comparison of the demonstrated disturbance types (changes of the fibre number of the input sliver Δz_i or changes of the velocity of the middle drafting godet pair Δv_z) shows that the disturbance dampening effect varies depending upon the disturbance type. Whereas an, as small as possible, draft of the draft in zone 1 is an advantage for a good evenness power effect of the drafting system at Δz_i-changes the inverted effect is valid for Δv_z-changes. A greater break draft in drafting zone 1 is more dampening for disturbances than a smaller break.

4.5 Necessary Measuring and Gauge Lengths to the Proof of Dynamic Disturbances in Yarns

The presentation until now has shown that dynamic disturbances of different kinds (periodic, aperiodic, at different technological operating points) of different process and product variables effect yarn disturbances along different yarn lengths. It should be questioned as to which basic totality of (at one working position) manufactured yarn length is to be included into a continuous or discontinuous test in the textile test lab. What cut length is to be selected for the continuous single tests to decisively describe dynamic disturbance effects in the yarn?

One can use a well-known rule of thumb for the electric measurement technique to technically prove test disturbances by means of discontinuous measurements. This is possible if the frequency of the tracing disturbance is known and if this frequency is suitable for a measurable effect to the yarn variable (for instance the fineness) according to the transfer and dampening properties of the system. The latter mentioned are to estimate simply by means of the amplitude frequency response or also roughly for the dominating system time constant T_c or for the critical frequency f_c.

The named rule of the electric measurement technique means that the carrier frequency of the amplitude modulation (a well-known procedure of the analogous transmission of electrical measuring signals) must be at least five times greater than the highest awaiting frequency of the measuring size. If this condition is fulfilled then a true to the form reproduction and transmission is given of the dynamic measuring size. This means, in other words, that the cycle duration for an oscillation of the carrier frequency must be included at least five times in the cycle duration of the shortest awaiting oscillation of the measuring size [5].

This rule (applied to the presented problem of the gauge and measuring length estimation) means that the yarn length (which has been exactly manufactured or processed during a full oscillation of the disturbance) is to be divided into at least five equal parts for further (for instance statistical) estimations.

If the disturbance frequency f and the take-down velocity v_o are known, then the *wavelength* of the disturbance λ_f in the fibre or yarn amounts to:

$$\lambda_f = \frac{v_o}{f} \tag{4.85}$$

The *necessary cut length* L_{cl} for the named single tests can be derived from Eq. 4.85 as follows:

$$L_{cl} = \frac{1}{n} \cdot \frac{v_o}{f} = \frac{\lambda_f}{n} \tag{4.86}$$

condition: $n \geq 5$

It is not enough to only select as *necessary gauge length* L_{gl} the yarn length of one cycle duration of the disturbance. Rather it is recommended that the basic totality of the gauge length L_{gl} to select be at least so large that five full disturbance oscillations are included. The *necessary gauge length* L_{gl} for fibre or yarn testings can be recommended consequently to:

$$L_{gl} = n \cdot \frac{v_o}{f} = n \cdot \lambda_f \tag{4.87}$$

condition: $n \geq 5$

According to Eqs. 4.86 and 4.87, 25 continuous single tests of yarn pieces with the cut length L_{cl} would be necessary to prove an expected disturbance frequency. Typical disturbance frequency ranges and the necessary yarn lengths L_{gl} and L_{cl} for their proof (which can be derived from the wavelength of a full disturbance oscillation λ_f in the shown manner) are collected in Table 4.4 for a row of disturbance causes in the polymer and glass spinning processes. Questions about the named aspects could not be answered if fixed standard gauge lengths or cut lengths were used (fineness testing 100 m or stress strain testing with specimen length of 0.5 m).

However, if the named conditions are fulfilled the following remarks are to be added according to the assertion of statistical characteristics as quadratic dispersion or variance and coefficient of variation. These characteristics do not express the absolute shifts around the mean values of the concerned variables in consequence to their integral calculation laws. If conditions are being observed for the decision of the yarn lengths L_{gl} and L_{cl} according to

Eqs. 4.86 and 4.87 (to investigate an appointed disturbance cause of known frequency f) then the coefficient of variation will show sinusoidal shifts of approximately 0.7 times around the mean value only (exactly $\sqrt{2}/2$ times) for real existing maximum shift amplitudes.

It has been shown in Sect. 2.5.2 that the disturbance frequency f of process and product variables essentially effect the interesting product variables of the final product only if
- the dynamic transmission behaviour is shown with a considerable transfer or amplification factor and
- the disturbance frequency f is located in an appointed range, which depends on the critical frequency f_c of the process line.

The last condition results in a practical undamped dynamic transmission of a cause disturbance to the effect variable by a *proportional action with delay of first order*

$$f \leq f_c \tag{4.88}$$

It should be remembered that proportional action with delay of first order takes place in the fibre formation of melt spinning for the transmission of Δv_o-, Δv_i-, $\Delta \varrho$- or Δq_i-disturbances to $\Delta T t_o$-shifts.

If *differential action with delay of first order* lies before, on the contrary then the condition reads for undamped disturbance transmission as:

$$f \geq f_c \tag{4.89}$$

Differential action with delay of first order exist for instance for Δl-disturbances, in melt spinning and its effect to $\Delta T t_o$-shifts.

In Table 4.5 time constants T_c and critical frequencies f_c (calculated by means of Eqs. 2.47 and 2.49 are combined on the basis of the output velocity v_{om} and length of the process line l_m) for some typical yarn formation and processing lines. The collection can support estimations to possible effects of periodic disturbances with known frequency f for variables of the yarn at the output of a yarn formation or processing line.

Table 4.4. Disturbance causes, disturbance frequencies and disturbance wavelengths in the fibre or yarn of melt spinning processes; necessary gauge and cut lengths for the prove of disturbances (v_{om} = take-down velocity in m/min)

Cause of the disturbances at the spinning equipment	Disturbance frequency f [Hz]	Wavelength in the fibre or yarn λ_f [m]	Necess. gauge length L_{gl} [m]	Necess. cut length L_{cl} at discontinuous testing [m]
Melt spinning of polymers				
Bobbin changing	(1.4...5.6) $\cdot 10^{-4}$	(12...3) $\cdot 10 \cdot v_{om}$	$\geq$ (6..1.5) $\cdot 10^{2} \cdot v_{om}$	$\leq$ (24...6) $\cdot v_{om}$
Melt temperature	(1.7...17) $\cdot 10^{-3}$	(10...1) $\cdot v_{om}$	$\geq$ (50..5) $\cdot v_{om}$	$\leq$ (20...2) $\cdot 10^{-1} \cdot v_{om}$
Oiling disk	(1.7...3.3) $\cdot 10^{-1}$	(10...5) $\cdot 10^{-2} \cdot v_{om}$	$\geq$ (5..2.5) $\cdot 10^{-1} \cdot v_{om}$	$\leq$ (2...1) $\cdot 10^{-2} \cdot v_{om}$
Spinning pump	(1.7...6.7) $\cdot 10^{-1}$	(10...2.5) $\cdot 10^{-2} \cdot v_{om}$	$\geq$ (5..1.25) $\cdot 10^{-1} \cdot v_{om}$	$\leq$ (20...5) $\cdot 10^{-3} \cdot v_{om}$
Quenching air	(5...50) $\cdot 10^{-1}$	(33...3.3) $\cdot 10^{-3} \cdot v_{om}$	$\geq$ (16.7...1.7) $\cdot 10^{-2} \cdot v_{om}$	$\leq$ (67...6.7) $\cdot 10^{-4} \cdot v_{om}$
Traverse motion	(1...10) $\cdot 10^{-1}$	(17...1.7) $\cdot 10^{-4} \cdot v_{om}$	$\geq$ (85...8.5) $\cdot 10^{-4} \cdot v_{om}$	$\leq$ (33...3.3) $\cdot 10^{-5} \cdot v_{om}$
Melt spinning of glass				
Bobbin changing	(5.7...16.7) $\cdot 10^{-4}$	(3...1) $\cdot 10 \cdot v_{om}$	$\geq$ (15..5) $\cdot 10 \cdot v_{om}$	$\leq$ (6...2) $\cdot v_{om}$
Main power (melt temp.)	$\leq 4 \cdot 10^{-1}$	≥ 4.2 $\cdot 10^{-2} \cdot v_{om}$	≥ 2.1 $\cdot 10^{-1} \cdot v_{om}$	≤ 8.4 $\cdot 10^{-3} \cdot v_{om}$
Throughput spinneret				
- without T_s-control	$\leq 1 \cdot 10^{-3}$	≥ 1.7 $\cdot 10^{1} \cdot v_{om}$	≥ 8.5 $\cdot 10^{1} \cdot v_{om}$	$\leq 3.4 \cdot v_{om}$
- with T_s-control	$\leq 1 \cdot 10^{-4}$	≥ 1.7 $\cdot 10^{2} \cdot v_{om}$	≥ 8.5 $\cdot 10^{2} \cdot v_{om}$	≤ 3.4 $\cdot 10 \cdot v_{om}$
- quick traverse	$\approx 1.751 \cdot 10^{1}$	≈ 9.5 $\cdot 10^{-4} \cdot v_{om}$	≥ 4.75 $\cdot 10^{-3} \cdot v_{om}$	≤ 1.9 $\cdot 10^{-4} \cdot v_{om}$
	$\approx 3.5 \cdot 10^{1}$	≈ 4.8 $\cdot 10^{-4} \cdot v_{om}$	≥ 2.4 $\cdot 10^{-3} \cdot v_{om}$	≤ 9.6 $\cdot 10^{-5} \cdot v_{om}$
- slow traverse	$\approx 3.3 \cdot 10^{-2}$	≈ 5 $\cdot 10^{-1} \cdot v_{om}$	$\geq 2.5 \cdot v_{om}$	≤ 1 $\cdot 10^{-1} \cdot v_{om}$

Table 4.5. Quantities of time constants and critical frequencies of different fibre formation and fibre processing process lines

Process step	Output velocity of the process step v_{om} [m/s]	Formation length of the process line l_m [m]	Time constant of the process line T_c [s]	Critical frequency of the process line f_c [Hz]
Man-made fibre manufacturing				
Spinning classically and spin-draw-winding	$(1.5...2) \cdot 10$	4...6	$(2...4) \cdot 10^{-1}$	$(8...4) \cdot 10^{-1}$
Spinning, high speed spinning	$(5...10) \cdot 10$	2...4	$(2...8) \cdot 10^{-2}$	8...2
Draw, classically	$(1.2...1.5) \cdot 10$	$3.5...4.5 \cdot 10^{-1}$	$(2.3...3.8) \cdot 10^{-2}$	6.9...4.2
Draw, spin-draw-winding	$(5...10) \cdot 10$	$4.5...5.5 \cdot 10^{-1}$	$(4.5...11) \cdot 10^{-3}$	$(3.5...1.5) \cdot 10$
False twisting, texturing	2.5...10	1...2	$(1...8) \cdot 10^{-1}$	$(16...2) \cdot 10^{-1}$
Yarn manufacturing				
Draw, slivers and rovings	1...8	$(1...5) \cdot 10^{-1}$	$(1.3...50) \cdot 10^{-2}$	12.2...0.32
Draw, ring frame	$(3...10) \cdot 10^{-1}$	$(5...20) \cdot 10^{-2}$	$(5...67) \cdot 10^{-2}$	$(32...2.4) \cdot 10^{-1}$